Stylet Penetration by Adult *Homalodisca coagulata* on Grape: Electrical Penetration Graph Waveform Characterization, Tissue Correlation, and Possible Implications for Transmission of *Xylella fastidiosa*

ELAINE A. BACKUS,[1] JAVAD HABIBI,[2] FENGMING YAN,[3] AND MARK ELLERSIECK[4]

ABSTRACT   The sharpshooter *Homalodisca coagulata* (Say) (Hemiptera: Cicadellidae: Cicadellinae) is an exotic vector of the Pierce's disease (PD) bacterium, *Xylella fastidiosa* (Wells et al.), that was first observed in California in 1989. *H. coagulata* has since greatly increased the threat of PD to the grape industry as well as stone fruit, nursery, and ornamental industries in California. This is the first in a series of articles that together describe how sharpshooter stylet penetration behaviors (especially intricate stylet activities, salivation, and ingestion) control transmission (i.e., acquisition and inoculation) of *X. fastidiosa*. Herein, we categorized and characterized alternating current electrical penetration graph (EPG) waveforms from glass-winged sharpshooter stylet penetration on petiole of susceptible grape ('Cabernet Sauvignon'), paying special attention to waveform fine structures that are likely to be the key to detecting the instant of inoculation. We also correlated waveforms with salivary sheath termini in grape tissues. For the first time in any EPG study of leafhopper or planthopper feeding, we demonstrate through case studies of individual probes how to follow the process of stylet penetration step by step as it is occurring, including salivary sheath branching and when the stylets first puncture a xylem cell. Finally, we discuss the implications of our findings for understanding the transmission mechanism of *X. fastidiosa*, in comparison with hypothesized mechanisms in the literature.

KEY WORDS   *Homalodisca coagulata*, electrical penetration graph, electronic monitoring of insect feeding, probing, Pierce's disease

THE SHARPSHOOTER, *Homalodisca coagulata* (Say) (Hemiptera: Cicadellidae: Cicadellinae), is an exotic, efficient vector of the Pierce's disease (PD) bacterium, *Xylella fastidiosa* (Wells et al. 1987) that was first sighted in California in 1989 (Sorensen and Gill 1996). *H. coagulata* has since greatly increased the threat of PD to the grape industry as well as stone fruit, nursery, and ornamental industries in California (NRC 2004). One of the best tactics for long-term management of the vector and disease will be host plant resistance. Resistance to both *X. fastidiosa* and to the vector's ability to transmit the bacterium is being actively sought (NRC 2004). However, progress in developing both types of resistance is severely impeded by a lack of fundamental understanding of *X. fastidiosa* transmission process, i.e., how, when, and in which cells the vector ingests and/or inoculates the bacteria. Also, the

details regarding exactly how vector feeding affects transmission efficiency and PD epidemiology are unknown.

This is the first in a series of articles that together answer these fundamental questions about how sharpshooter feeding controls transmission (i.e., acquisition and inoculation) of *X. fastidiosa*. The long-term goals of our research are, first, to analyze the intricate details of stylet penetration (also known as probing). In particular, we seek to identify the instant of bacterial inoculation during the feeding process, in real time. Second, we plan to synthesize these details into a comprehensive model of feeding behavior and physiology that will explain the mechanisms of *X. fastidiosa* transmission and the role of feeding in transmission efficiency. Ultimately, we plan to apply this model to the development of a stylet penetration index (Serrano et al. 2000), an experimental and analytical technique for rapid, nondestructive and high-throughput screening of plants. In this way, breeders can determine whether or to what degree a certain genotype will stimulate the vector to feed in a manner that will acquire and/or inoculate the bacterium.

Electrical penetration graph (EPG) monitoring of insect feeding allows highly rigorous detection, quan-

[1] USDA–ARS Crop Disease, Pests and Genetics Research Unit, San Joaquin Valley Agricultural Sciences Center, Parlier, CA 93648.
[2] Department of Entomology, University of Missouri, Columbia, MO 65211.
[3] College of Life Sciences, Peking University, Beijing, China.
[4] Department of Statistics, University of Missouri, Columbia, Columbia, MO 65211.

tification, and analysis of the stylet penetration behaviors of any piercing-sucking arthropod on an electrically conductive feeding substrate. First invented by McLean and Kinsey (1964) then substantially improved by Tjallingii (1978), the technique has been extensively reviewed recently (Ellsbury et al. 1994, Walker and Backus 2000). Most work to date has studied plant-feeding hemipterans and thysanopterans (Backus 1994; Walker and Backus 2000, and references therein). A test insect is attached to the EPG monitor through a gold wire glued to it with conductive paint. The insect is then placed on a plant with an output electrode from the monitor's voltage source in its soil. When the insect's stylets penetrate into the plant, the circuit is closed. Changes in voltage across the input resistor (electrically modeling the stylets) are amplified and recorded as waveforms for later measurement and analysis (Walker 2000). The only EPG studies of any sharpshooter species previous to this work are two studies of the sharpshooter *Graphocephala atropunctata* (Say) (Crane 1970, Almeida and Backus 2004), a native California vector of *X. fastidiosa* that was the most important vector in California until the introduction of *H. coagulata.*

The main objective of the current study was to identify and define the alternating current (AC) EPG waveforms from adult *H. coagulata* feeding on susceptible grape petioles, that is, to 1) categorize and electrically characterize the waveforms, paying special attention to waveform fine structures that are likely to be the key to detecting the instant of inoculation, and 2) determine the biological meanings of these waveforms. Such correlations must always be performed when a new species is recorded for the first time. Abstract EPG *waveforms* are defined by correlation with *stylet location* in the plant as well as the intricate *stylet activities* performed therein. This three-way definition is termed the "triangle of correlations" (Backus 1994, Walker 2000). Herein, we used histology of salivary sheaths in probed plant tissues to correlate waveforms with stylet locations. Insights from our study of waveform fine structure and sheath anatomy, combined with results from a companion study of *H. coagulata* feeding in artificial diets (Joost et al. 2006), correlate waveforms with stylet activities, plus activities with location. Also, for the first time in any EPG study of leafhopper or planthopper feeding, we demonstrate herein through case studies of individual probes how to follow the process of stylet penetration step by step as it is occurring, including salivary sheath branching and when the stylets first puncture a xylem cell. Finally, we briefly discuss the implications of our findings for understanding the transmission mechanism of *X. fastidiosa*, a gram-negative, plant pathogenic bacterium that can live only in the xylem cells of plants and the foreguts of its vectors, xylem-feeding auchenorrhynchan hemipterans (Purcell and Hopkins 1996). The bacterium is the only known pathogen that is propagative yet noncirculative in its vector.

Materials and Methods

Insects and Plants. Adult sharpshooters were field collected from citrus at Agricultural Operations, University of California, Riverside, and shipped overnight to the University of Missouri, Columbia, where laboratory studies were performed. Insects were caged on greenhouse-grown chrysanthemum, *Dendranthema grandiflora* Tzvelev 'White Diamond' in a quarantine growth room at 29–32°C and a photoperiod of 14:10 (L:D) h. Both male and female field-caught insects were used for EPG recordings. Degree of *H. coagulata* infectivity with *X. fastidiosa* was unknown. One to 2 d before correlation experiments were performed, test insects were transferred to grape plants, *Vitis vinifera* 'Cabernet Sauvignon' for pretest conditioning. Grapevines had been grown previously from cuttings provided by Foundation Plant Material Services, University of California, Davis, and reared in a greenhouse under supplemental lighting (photoperiod of 14:10 [L:D] h). Plants used were 4–8 wk past the start of leafing.

EPG Protocols, Equipment, and Data Acquisition. AC EPG recordings of *H. coagulata* were carried out as for *G. atropunctata*, described in detail in Almeida and Backus (2004). In brief, sharpshooters were held by hand with an "abdomen"-type aspirator (i.e., a Pasteur pipette flame-glazed to fit snugly around the abdomen), tethered with silver conducting paint (Ladd Research Industries, Burlington, VT) and 50-μm (0.0020-in.)-diameter gold wire (Sigmund Cohn, Mount Vernon, NY), and allowed to acclimate to the wire for 1–5 h on a grape petiole. Insects were then starved while dangling from the wire for 1–3 h before recording. *H. coagulata* were EPG monitored for varying times (10 min to 30 h) by using an AC Missouri Monitor (Backus and Bennett 1992), version 2.2 (modified from the published version with higher amplification and larger-value coupling capacitors for better passage of DC offsets). Input impedance on this monitor is a fixed level of 10^6 Ohms. All recordings were performed in a Faraday cage, with 100-mV, 1,000-Hz substrate voltage applied to the soil of intact grape plants. Output waveforms were digitized at 100 samples per second by using a DI-720 analog-to-digital board, WinDaq Pro+ software (Dataq Instruments, Akron, OH) and Microsoft Excel as described in Almeida and Backus (2004). By convention and for ease of measurement, a waveform event was measured only if its duration exceeded 2.0 s.

Waveform Characterization and Biological Correlations. For experiment 1, EPG recordings were made from ≈200 insects, one at a time for 1–24 h, at all times of day, while they were probing the succulent petioles of young grape leaves. Probes were all naturally terminated by the insect and were used to preliminarily categorize and electrically characterize specific waveforms phases, families and types (see *Results* below for definitions). Windaq allows waveforms to be amplified in voltage by using gain steps from 1 to 512× as well as compressed or expanded in time for examination at coarse (>10 s/cm, or Windaq compression of

>13), medium (4–10 s/cm, compression of 5–12), and fine structure (0.20–3.8 s/cm, compression of 1–4) levels (described more fully in Almeida and Backus 2004). Excretory droplet production and rate were observed and visually correlated with waveforms to determine which corresponded with ingestion.

For experiment 2, an additional 42 insects were used for histological correlation of waveforms with location and structure of salivary sheaths; each recorded on its own, fresh grape plant. Stylet penetration was artificially terminated in mid-waveform by abruptly but carefully pulling the insect off the plant by its wire. Waveforms A1, B2, C, and N could be identified during real-time display, so truncation of those waveforms could be planned as they occurred. However, waveforms A2, B1, and B2m could not be distinguished from one another at the time of performance, because of their small size (amplitude) in real-time display and/or rapidity of performance. For these three waveforms, therefore, several probes were terminated during likely A2/B1/B2m events, and later postacquisition examination of waveforms allowed us to determine during which waveform the probe was actually truncated. After termination, the probe site was marked with ink, as described in Almeida and Backus (2004) and a 1.0–2.0-mm block of petiole tissue surrounding the presumed salivary sheath was then excised and fixed for histological processing, according to methods in Serrano and Backus (1998) and Ruzin (1999). Briefly, tissues were fixed in CRAF III (Ruzin 1999) overnight, dehydrated in a graded series of tertiary butyl alcohol, embedded in Paraplast (Fisher, St. Louis, MO), serial sectioned at 10 μm, mounted on slides by using 5% ammonium hydroxide (Fisher), stained with aqueous saffranin O and then counterstained with ethanolic fast green, and coverslipped using Permount (Fisher). Slides were examined and images were collected using an Olympus IX 70 compound microscope and its attached digital camera. Images were processed using Image Pro+ (Media Cybernetics, San Diego, CA) version 5.0 on a Dell XPS 8733r computer. Thirty four of the 42 plant tissues excised for histology (81%) contained recoverable salivary sheaths.

Statistical Analysis. Descriptive and analytical statistics of waveform events from experiment 2 were performed as described by Almeida and Backus (2004) and Serrano (1997) by using SAS (SAS Institute 1998). Measurement variables and heuristic analysis levels are defined and described in more detail in Serrano (1997), Serrano et al. (2000), and Almeida and Backus (2004). Terminology used was as in Backus (2000). In brief, stylet penetration (probing) is defined as all feeding behaviors performed during a probe; a probe is defined as the duration of time from the start of stylet penetration until stylet withdrawal. A waveform event is the duration within a probe during which an uninterrupted waveform is performed; therefore, a probe consists of an unbroken sequence of waveform events.

All salivary sheaths (regardless of whether branch tips were hollow or filled; see definition and explana-

tion below) were categorized as single- or multibranched. All waveform events within these probes were sorted first by waveform and then by single-versus multibranched sheaths. Then, the total number of events (TNE) (i.e., for the whole cohort), mean waveform duration per event (WDE), total number of insects for each waveform type (TNIw), and mean number of waveform events per insect (NWEI) (the same as mean number of waveform events per probe [NWEP], because only one probe was made per insect) were calculated for each waveform type. For calculation of WDE, all experiment 2 events were used except the final, truncated events, because the latter were not naturally terminated. For calculation of mean NWEI, all experiment 2 events were used. Square root-transformed WDE and NWEI were compared between single- and multibranched sheaths for each waveform type by using analysis of variance (ANOVA), with subsequent pairwise comparisons made using Fisher's protected least significant difference (LSD) (PROC GLM) (SAS Institute 1998). Differences were considered significant at $\alpha = 0.05$. Experiment 2 probes were used for measurements of repetition rates of waveforms. Usually, five to 10 waveform events for each type were averaged. Repetition rate (also called waveform frequency) is the number of times a stereotypical waveform pattern (e.g., a certain type of peak) is repeated per sec (i.e., in Hertz).

Results

Waveform Categories: Phases, Families, and Types

Following a naming convention first developed by Tjallingii (Reese et al. 2000, van Helden and Tjallingii 2000) and described in detail in Almeida and Backus (2004), we used a hierarchical set of waveform categories. The waveform phase denotes the broadest behavioral categories such as pathway versus ingestion behaviors and can be easily distinguished even when the waveform is highly compressed to view overall, coarse structure. Phases are equivalent to the broad waveform designations used in early AC EPG studies (McLean and Kinsey 1967), such as salivation (now named pathway) and ingestion. Phase names that incorporated amplitude levels, used in Almeida and Backus (2004), have been shortened by dropping amplitude levels (e.g., high-amplitude/pathway phase has become pathway phase), because new correlations described herein have confirmed the relationship between amplitude and behavior. Additionally, a new phase has been identified and named interruption phase (see below). At medium resolution, more waveform details can be seen. Waveforms with related appearances and biological meanings were alphabetically designated as waveform families (i.e., A, B, C, and N). When the waveforms were further expanded to examine fine-structure detail, they were categorized to waveform type and designated numerically within family letters (i.e., A1, A2, B1, B2, and so on). In a few cases, subtypes also were categorized and designated by lowercase letters (i.e., B1s). Sequential

letter and number designations were chosen to represent partially sequential behaviors. However, *H. coagulata* exhibit flexibility and do not always perform the behaviors sequentially.

When describing waveform position and amplitude herein, we return to earlier EPG conventions and discard new terms defined in Almeida and Backus (2004). We define voltage level as the approximate position of a waveform type relative to the on-plant baseline (0%) and the top of the highest peak in the probe (100%). In contrast, amplitude is the actual size, from peak to valley, of the waveform, and can be expressed either in volts (i.e., absolute amplitude) or percentage (similar to voltage level) (i.e., relative amplitude) (note that absolute and relative amplitude are defined differently herein, compared with Almeida and Backus 2004).

AC Waveform Characterization and Excretory Droplet Correlations

Table 1 summarizes all waveform characterization and correlation data discussed in this article.

Pathway Phase: A Waveforms. *Waveform A1* is characterized by moderately regular, high-amplitude, very slow peaks at the immediate beginning of the probe (Fig. 1a, unlabeled; b and c, labeled; Table 1). These peaks are usually the highest amplitude waveforms of the probe; thus, their peaks mark the 100% voltage level. The A1 valleys between peaks are offset from the lowest probing voltage level, so that A1 is superimposed on a distinct, hump-like waveform base far above baseline. Therefore, waveform position is offset ≈30–50% above the base (Fig. 1a and b). Typically, two to 12 discrete A1 peaks occur in rapid succession, and each peak is ≈0.5 s in duration. Interestingly, individual A1 peaks almost always are separated by brief B1s waveform events (see description of B1 below) of about the same or longer duration, at the bottom of the A1 valleys (Fig. 1c).

Waveform A2 is somewhat different in appearance from A1 (Fig. 1b and d), being variable in both repetition rate and amplitude (Table 1). Usually, A2 is wave-like, very small in amplitude (5–10%), and highly irregular in appearance (Fig. 1b and d). At times, however, it also can manifest two regular portions. First, short peaks can occur that are like A1 peaks but usually smaller in amplitude (15–20%), fewer in number, and not offset on top of a large waveform hump (Fig. 1b, also compare c and d). Second, A2 is the only waveform occasionally displaying rapid, distinct decreases in voltage (Fig. 1d, starred arrow) that fall and then return to the previous voltage level in ≈1 s (Fig. 1d). The overall voltage level of A2 events usually declines gradually as the probe lengthens. However, it is not uncommon for A2 to occur at any voltage level, i.e., rising, falling or remaining stable. Short events of B1s also occur intermittently among A2 events, as with A1 (Fig. 1d).

Pathway Phase: B Waveforms. *Waveform B1:* Like A2, B1 can variably occur at any voltage level: rising, falling, or stable. Unlike A2, however, the fine structure of B1 is highly uniform, consisting of two subtypes. First, subtype B1s consists of rapid, very high-frequency "spikelet bursts" (Table 1) with very low amplitude (1–5%). These spikelet bursts (Fig. 1b, inset) are interspersed with the second subtype, B1w, composed of essentially flat or wave-like, irregular, interspike events (termed "waves"; Fig. 5b, blue inset box). B1 (especially B1s) is the only *H. coagulata.* waveform that is interspersed throughout all pathway events, occurring between most A1 and A2 peaks at the start of the probe (Fig. 1c), as part of B2 episodes (see below), and even sometimes during C (see below).

Waveform B2: B2 is very different in appearance from the A waveforms or B1. B2 is a highly uniform waveform that is composed of repeated smooth peaks. The peaks occur in highly stereotypical, distinct events shaped like upside-down chevrons (Figs. 1b, inset box, and 5b, yellow inset box) that can be repeated consecutively. Occasionally, only half of a chevron is made, when the B2 event is apparently aborted before completion (Fig. 5d). B2 usually occurs at a stable voltage level; however, it also can occur during declining voltage (Fig. 5d) and, more rarely, ascending voltage levels.

Waveform B2m: B2m is a much smaller-amplitude, shorter-duration, "micro" version of the B2 waveform, with the same frequency and similar appearance (Fig. 6b, blue inset box). Voltage levels are the same as for B2. However, the peaks are very short and not as complex and symmetrical as those of B2. Most B2m events were very short, <2 s in duration, and thus were not measured and included in data in Tables 2 and 3. However, when their event durations exceeded 2 s, they were measured.

Ingestion Phase: C Waveform. C is a highly stereotypical and repetitive pattern at very low amplitude (Table 1) and position that can continue with only brief interruptions for many minutes to hours at a time (Fig. 1a, inset; b). Slight variations in fine-structure appearance of the C waves occur as time progresses, from event to event (e.g., compare appearances of enlarged insets in Fig. 4). C waveforms were always interrupted by short events of waveform N (described below under "Interruption Phase"), causing the ingestion phase to be divided into 1stC, 2ndC, 3rdC, 4thC, and so on (Fig. 1b). C events with orders greater than fourth were combined in this study and called >4thC (Table 2). Combination of higher order events was done because most probes were terminated before 4thC; C was allowed to randomly continue beyond 4thC in only a small number of probes (Table 2).

Excretory droplets were observed to occur during C, in at least 20 probes (out of at least 60 probes that produced C) during experiment 1. Time at onset of excreta production was not noted (Fig. 4), although it was never within the first ≈5 min. Droplet production was directly observed relatively rarely because most probes were very short because of artificial termination, or long probes occurred at night. When droplet production was directly observed, it eventually developed a continuous, sustained rate of ≈1 droplet per

Table 1. Current definition of AC EPG waveforms for *H. coagulata*

Waveform name				Waveform characterization				Biological meaning	
Phase	Family	Type	Subtype	Voltage level (%)[a]	Absolute amplitude (%)[a]	Rep. rate[b]	Description	Stylet tip location	Stylet activity[c]
Pathway	A	A1		50–70	30–50	0.5 ± 0.01 (n = 10)	Highest amplitude waveform; peaks on top of hump-like voltage rise; always at the beginning of a probe	Epidermis, parenchyma/mesophyll	Formation of salivary sheath trunk; extension/retraction of entire stylet fascicle; secretion of watery saliva
		A2		35–40	5–25	Irregular	Medium-amplitude waveform; irregular with occasional small peaks, trenches and/or voltage declines	Parenchyma/mesophyll	Lengthening, polishing or hardening of salivary sheath; some watery salivation
	B	B1	B1s	20–50	5–10	17.1 ± 0.16 (n = 8) (range 15–24)	Single, very small spikelets, or highly uniform bursts of multiple spikelets; termed spikelet bursts	Parenchyma/mesophyll, pith, phloem, xylem	Ubiquitous throughout all pathway and interruption waveforms and occasionally in ingestion also. Coincident with maxillary stylet fluttering, but not synchronous with it; precibarial valve movement?
			B1w			Irregular	Brief, flat to wavelike events, interspersed between events of B1s	Same as B1s	Secretion of sheath saliva; stylets motionless?
		B2		20–40	10–15	3.0 ± 0.03 (n = 10)	Highly regular, stereotypical pattern of peaks that together form a chevron or half-chevron shape; usually in distinct episodes including B1s before and after B2 chevron	Parenchyma/mesophyll, pith	Highly stereotypical maxillary stylet sawing; used to exit hardened sheath or cut thru tough plant tissue; allows extension or branching of sheath; sheath salivation
			B2m	25–50	8–10	4.2 ± 0.09 (n = 4)	"Micro" version of B2; small chevrons usually less than 2 s in duration	Parenchyma/mesophyll, pith	Similar to B2, but less vigorous stylet sawing; sheath may be less hardened, or plant tissues softer?
Ingestion	C			5–8	2–5	0.4 ± 0.01 (n = 10)	Highly regular, stereotypical pattern of plateaus and valleys; smallest waveform	Usually xylem, rarely phloem	Ingestion of fluids into the cibarium, esophagus and beyond, via contraction of the cibarial dilator muscles; no salivation?
Interruption	N	Nonpathway		20–30	5–10	Irregular	Highly irregular, intermittent peaks and waves	Xylem	Secretion of watery saliva?
		Pathway-like (pathway name starts with N)		5–20	3–15	Regular	Similar to pathway waveforms of same name, but sometimes lower repetition rate (see text for rates)	Parenchyma/mesophyll	Similar to pathway waveforms of same name, but in deeper plant tissues

[a] Defined in text.

[b] Repetition rate, in Hertz; defined in text.

[c] Stylet activities summary is a combination of results from this study and Joost et al. (2006).
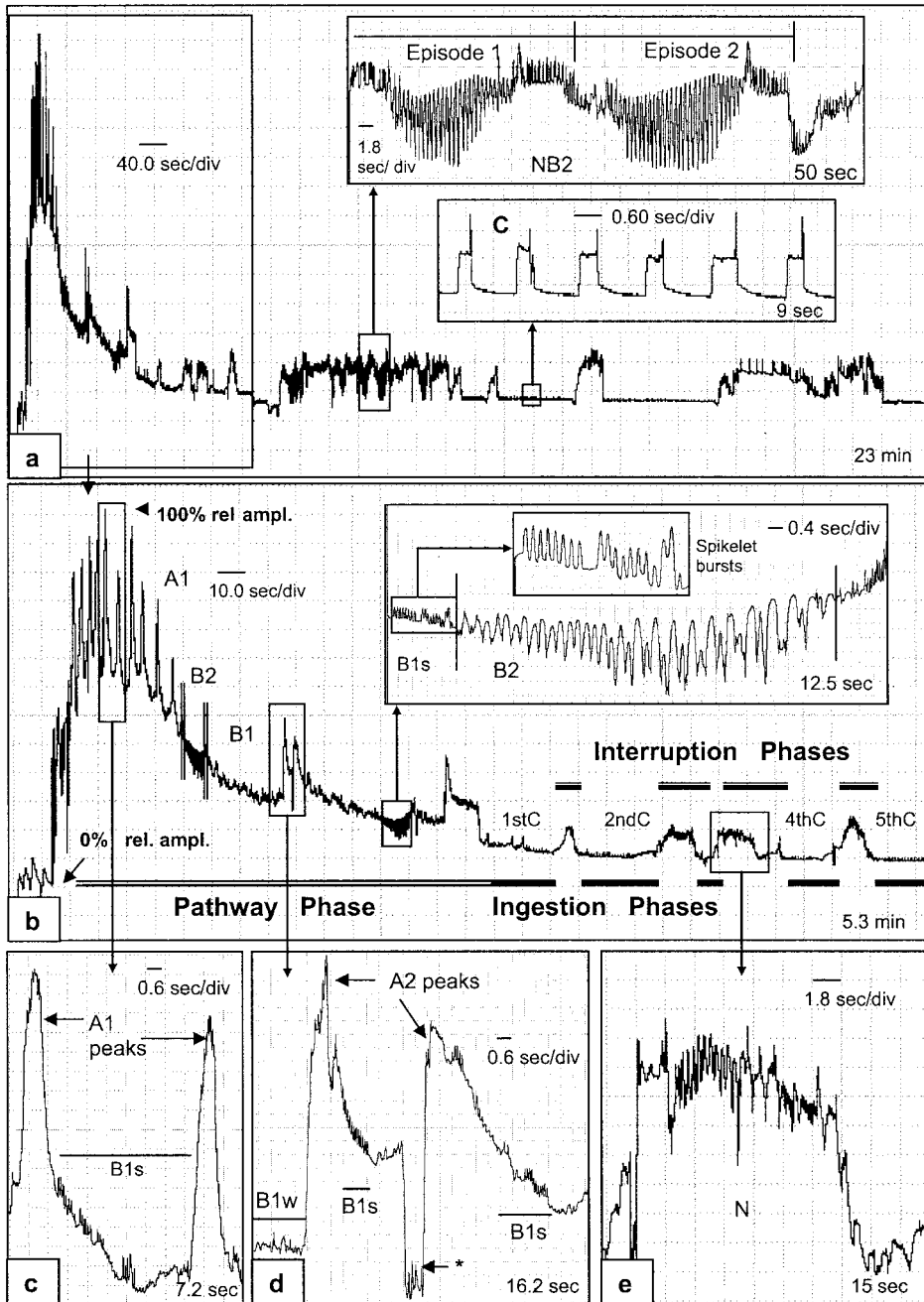
Fig. 1. Example EPG waveform traces representing stylet penetration by adult *H. coagulata* on susceptible grape petiole. Results from experiment 1. (a) Coarse-structure view of one probe, with insets showing amplified (y-axis) and expanded (x-axis) views, to reveal the fine structure of selected interruption and ingestion waveforms. Box around the pathway and early ingestion events is expanded in b. (b) Medium-structure view of pathway and early ingestion and interruption phases, with insets again showing amplified and expanded views of some waveforms. Boxed waveforms are also amplified and expanded in c–e. (c) Fine structure of A1 waveform type with intervening events of B1s. (d) Fine structure of A2, showing rapid decrease in voltage (*) and intervening B1s event. (e) Amplified and slightly less expanded view of nonpathway N.

second. C was the only waveform during which any excreta were produced. Thus, C clearly represents ingestion.

Interruption Phase: N Waveforms. The N waveform family represents a diverse mixture of waveforms that occur interspersed among waveform events of inges-

Table 2.   Key findings for the 24 single-branched sheaths and six hollow (*), final branches from multi-branched sheaths whose tip positions in plant tissue were definitively correlated with each waveform type listed

Sheath no.	Correlated waveform	Correlated cell type	Time to waveform	Event duration	Saliva in cell?	Branch resent?
25	A1	Collenchyma	4.1	3.2	No	No
27	A2	Interfascicular parenchyma	35	3	Yes	Yes
2	B1	Phloem	11.4	2.1	Yes	Yes
1	B1	Cortical parenchyma	17	7.5	Yes	No
3	B1	Collenchyma	20.5	6.7	?	No
19	B1	Interfascicular pith	21.7	11.1	Yes	Yes
24	B2	Cortical parenchyma	24.7	5.9	Yes	Yes
12	B2	Interfascicular pith	46.7	7.9	Yes	Yes
6	B2	Pith	66.8	6.5	Yes	Yes
4	B2	Interfascicular parenchyma	89.2	5.1	Yes	No
23	1stC	Phloem	28.8	82.4	Yes	Yes
11	1stC	Xylem vessel element	32.9	17.6	Yes	Yes
34	1stC	Xylem vessel element	45.1	299.3	No	Yes
9	1stC	Other xylem	52.2	10.7	No	Yes
30	1stN(B1)	Pith	148.5	9.4	Yes	Yes
31	1stN	Xylem vessel element	108.1	8.9	No	Yes
7	2ndC	Protoxylem	56.7	3	No	Yes
21	2ndC	Other xylem	67.5	20.2	No	Yes
5*	2ndC	Xylem vessel element	89.1	12.6	No	Yes
15	2ndN	Xylem vessel element	338.2	4.9	No	Yes
18	3rdC	Xylem vessel element	151.8	708	Yes	Yes
20*	3rdC	Xylem vessel element	221.6	1134.1	Yes	Yes
16	3rdC	Other xylem	272.1	17	No	Yes
8	4thC	Xylem vessel element	135.8	29.3	Yes	Yes
13*	4thC	Xylem vessel element	327.4	37	Yes	Yes
29	4thC	Xylem vessel element	371.1	340.8	No	Yes
28*	4thC	Xylem vessel element	490	377	Yes	Yes
33	4thNB1	Xylem vessel element	1,657.2	14.3	Yes	Yes
17*	>4thC	Xylem vessel element	284.3	24.9	No	Yes
26*	>4thC	Xylem vessel element	611.1	12	No	Yes
10	>4thC	Xylem vessel element	8,566	570	No	Yes

Sheaths are sorted by correlated waveform and then by time to waveform.

tion, i.e., interrupting the otherwise continuous C waveform. There are two types of interruption phase waveforms.

Nonpathway-Like N. When interruption waveforms do not resemble pathway-like waveforms, they are designated by the letter N alone. This waveform is highly variable in appearance, with both uniform and nonuniform portions (Fig. 1e), but not clearly resembling any of the above-described pathway waveforms.

Pathway-Like N. When clearly recognizable, pathway-like waveforms are embedded within interruption phase (e.g., NB2 in Fig. 1a, inset), designations consist of N preceding other pathway waveform designations, i.e., NA1, NA2, NB1, and NB2. Like C events, N events also were categorized by the order they

occurred in the probe, i.e., 1stN, 2ndN, 3rdN, and so on. In that case, we sequentially numbered all N events, regardless of whether they contained pathway activities. Therefore, e.g., 3rdNB2 would be defined as the third N event of any type, which in that case happens to resemble B2; it would not mean the third N event of the B2 type.

Salivary Sheath Correlations with Waveforms

Anatomy of a Salivary Sheath. *H. coagulata* salivary sheaths had a distinctive and stereotypical bush-like anatomy, similar to those of other leafhoppers. The basal-most portion of the sheath was wide, usually triangular, very thick-walled, and always at least par-

Table 3.   WDE (mean ± SD) in seconds, for each C event order

C event order	All sheaths combined	Single-branched sheaths		Multibranched sheaths		P value
	WDE	WDE	n	WDE	n	
1stC	21.8 ± 16.3	24.8 ± 19.6	10	18.6 ± 11.7	9	0.8551
2ndC	57.3 ± 60.4	91.8 ± 68.3	7	27.1 ± 32.4	8	0.1136
3rdC	178.4 ± 315.8	80.9 ± 86.0	5	248.0 ± 405.4	7	0.1255
4thC	201.75 ± 204.2	337.5 ± 329.9	2	156.5 ± 163.6	6	0.1230
>4thC	706.3 ± 717.5	1123.9 ± 603.0	8	38.04 ± 28.4	5	<0.001

Only durations of naturally terminated events are used. Events are combined for all sheaths as well as broken out by sheath type (single-branched vs. multibranched). *P* values are from pairwise LSD comparisons of WDE for each C event order, between single- and multibranched sheaths, at $\alpha = 0.05$.

tially hollow. This portion was designated the sheath trunk. From the apical end (i.e., tip) of the trunk, single or multiple branches of the sheath would extend into deeper plant tissues. (In this work, "branch" refers to any, usually narrow and thin-walled extension of the salivary sheath beyond the sheath trunk. Because such branches are always made by the unique actions of the maxillary stylets alone, we will not use the term "unbranched" sheath unless the trunk was the only part of the sheath made.) The trunk tip usually was located just outside the vascular tissue, in the grape petioles studied. Sheath branches were variable in width, wall thickness, and whether they were hollow or filled with sheath saliva. However, they almost always had a smaller diameter than the sheath trunk. Branches were formed as the maxillary stylets penetrated past the mandibular stylets, more deeply into the vascular tissues and beyond, into the pith.

Definitive Correlation of Waveforms with Sheath Tips in Plant Cells. Of the 34 recovered salivary sheaths, 24 were found to be single-branched sheaths and 10 were multibranched sheaths (five double- and five triple-branched). Definitive correlation of a recorded waveform with the salivary sheath tip's location depended on identifying which branch of the sheath was the final branch. This was straightforward in the case of a single-branched sheath, but it could have been difficult in multibranched sheaths. However, in most instances, such identification was accomplished in the following manner. When stylets were forcefully removed from the plant, the insect usually was not given enough time to fill the plant cell and its salivary sheath upon withdrawal (the latter is a normal behavior for most sheath-feeding auchenorrhynchans; E.A.B., personal observation). In most cases, the waveform was cleanly terminated, i.e., the waveform abruptly fell to baseline, without a "pull-out spike" (indicating brief salivation) or any other waveform intervening (Fig. 5d). Thus, the final sheath branch made was usually distinctly hollow (Fig. 5c, arrow 5). Almost all sheath branches that were not smoothly hollow were filled, and their terminal vascular cells were occluded with bluish staining saliva (Fig. 6a, arrow 3). Table 2 shows data from all 24 single-branched sheaths, plus six final, hollow sheath branches from multibranched sheaths (Table 2, indicated by bold font). Additional cell types at the putative termini for filled sheath branches are described below and their data were used in Table 4 for comparison, but they were not considered definitive.

Pathway Phase: A Waveforms. The A waveform family represents the major secretion of sheath saliva and formation of the salivary sheath, especially the trunk and thicker branches.

Waveform A1: Out of the seven probes artificially terminated during A1, only one sheath was found intact within sectioned plant tissue (Table 2). This successfully interrupted probe lasted only 3.2 s. Its corresponding sheath was very shallow, thin-walled, and did not reach vascular tissue. It was less than one-third the length of a typical sheath trunk and

Table 4. TNE, WDE, TNIw, and NWEI for reach waveform type, divided into those for single-branched versus multibranched sheaths

Wf[a]	No. of branches	TNE	WDE (mean ± SEM)[b]	TNIw	NWEI (mean ± SEM)[b]
A1	Single	46	6.83 ± 0.93	24	1.96 ± 0.23
	Multi	26	11.02 ± 4.42	10	2.6 ± 0.45
A2	Single	30	6.48 ± 1.76	21	1.48 ± 0.18
	Multi	18	6.19 ± 1.35	10	1.8 ± 0.29
B1	Single	51	7.27 ± 0.81	23	2.39 ± 0.24
			*		*
	Multi	41	12.71 ± 2.39	10	4.10 ± 0.91
B2	Single	3	8.13 ± 0.72	4	1.75 ± 0.25
	Multi	13	7.52 ± 0.35	8	1.63 ± 0.38
B2m	Single	1	2.40	1	1.00
	Multi	3	4.10 ± 0.91	2	1.50 ± 0.50
C	Single	33	332.77 ± 94.82	14	3.22 ± 0.76
			*		*
	Multi	30	55.55 ± 15.25	9	4.22 ± 0.62
N	Single	26	12.54 ± 1.70	10	2.70 ± 0.96
	Multi	24	8.20 ± 0.87	9	2.78 ± 0.60
NA2	Single	0		1	
	Multi	1	13.60	1	1.00
NB1	Single	4	10.13 ± 1.38	1	5.00
	Multi	3	16.40 ± 4.80	2	1.50 ± 0.50
NB2	Single	2	8.30 ± 0.20	1	2.00
	Multi	3	8.37 ± 1.29	2	1.50 ± 0.50
NA1	Single	2	7.55 ± 0.55	1	2.00

For WDE, only durations of natural terminated events were used.
[a] Wf, waveform.
[b] An asterisk between two values in a column signifies they are significantly different at $\alpha = 0.05$.

terminated in cortical parenchyma (Fig. 2a) above a vascular bundle.

Waveform A2: Only one attempt succeeded in disturbing stylet penetration during a fleeting, 3 s A2 event immediately after a small voltage peak 35 s into the probe (Table 2). The sheath was recovered; however, the peripheral part of its trunk suffered fixation artifacts. Enough was salvageable to show a fully formed trunk plus a small, single branch that terminated in interfascicular parenchyma between two vascular bundles at the depth of the neighboring xylem (Fig. 2b). A small bubble of sheath saliva inside the parenchyma cell suggests that the stylets were caught in the process of secreting sheath saliva (Fig. 2b, arrow).

Pathway Phase: B Waveforms. The B waveform family represents the final stages of pathway phase, especially very thin-walled sheath branching on the way to, just before, or immediately after entry into or exit from a vascular cell.

Waveform B1: Four correlatable salivary sheaths were recovered successfully from probes disturbed during B1 very early (Table 2). These probes were 10–22 s into pathway before B1 began and 2–11 s of B1 elapsed before termination. Terminal cell type and depth of penetration varied for the four probes (Table 2), but all were in nonxylem tissues. Three of the four sheaths had a small deposit of sheath saliva at their tips (i.e., sheath 1, 2, and 19). Sheaths 1 (Fig. 2e) and 2 (not pictured) apparently injected large but amorphous deposits of sheath saliva into the cells; sheath 19 (Fig. 2f–h) injected a small, discrete ball of saliva (best
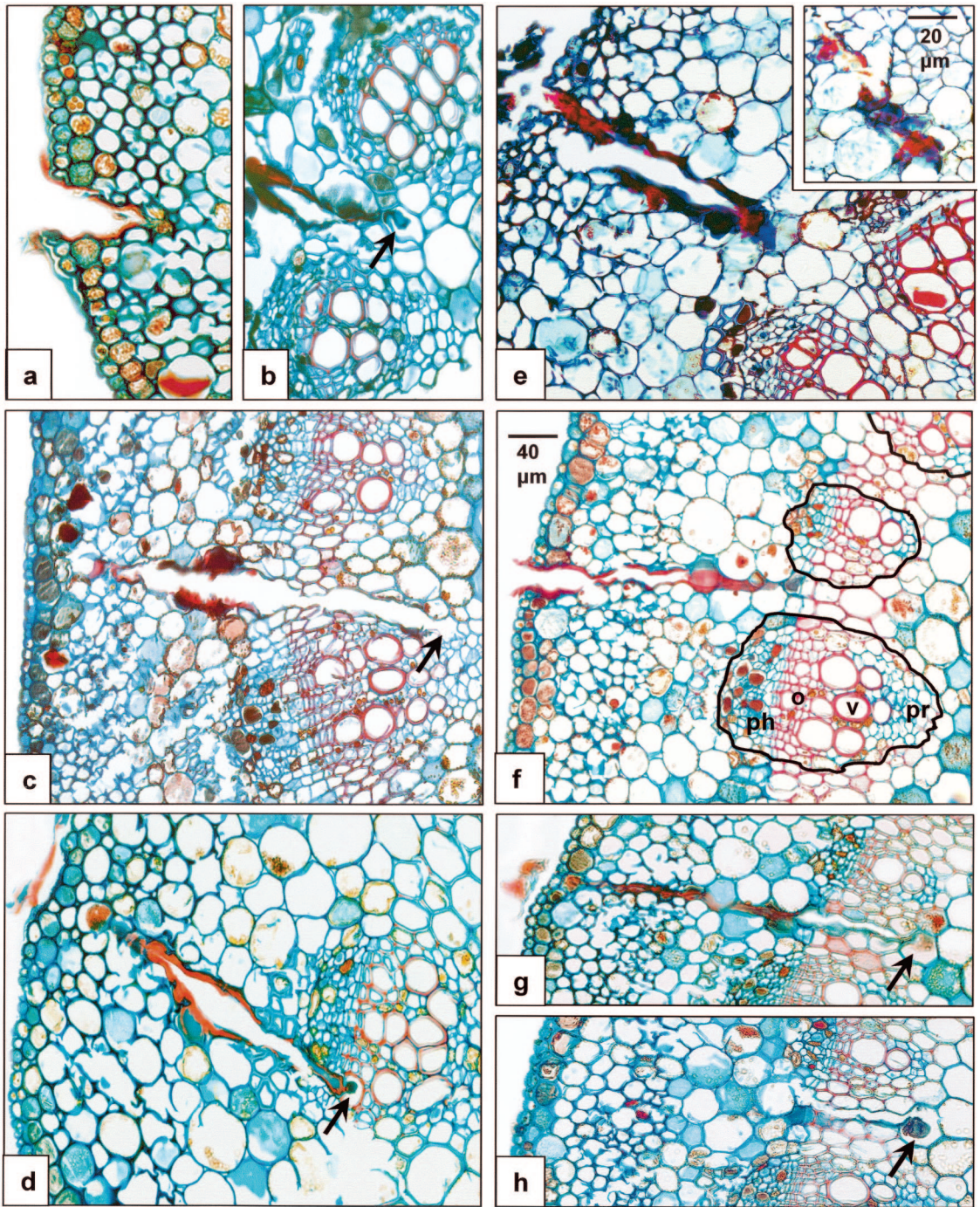
Fig. 2. Composite plate of selected salivary sheaths from experiment 2. All images are at 20× original magnification, except the inset of e, which is at 40×. (a) Sheath trunk left when insect 25's probe was terminated after 3 s. The remaining images show sheaths at various stages of formation (see text) from the following insects' probes: b, 27; c, 7; d, 33; and e, 1. (f–h) Three consecutive sections through the sheath of insect 19. f exemplifies the anatomy of young grape petiole's vascular bundles (outlined in black); ph, phloem; o, other xylem (small red cells); v, xylem vessel elements (large, thick-walled, red cells); pr, protoylem (small blue cells).

visible in Fig. 2h) into the cell. The fourth B1-terminated sheath (from insect 3, not pictured) consisted of a large, amorphous deposit of sheath saliva, shallowly placed in the plant.

Waveform B2: Four salivary sheaths from probes artificially terminated during B2 were recovered. The four B2 events occurred 25–89 s into the probe and lasted for 5–8 s (Table 2). The termini of their sheaths were in nonvascular parenchyma or pith cells. Strikingly, all four terminated sheaths ended in at least one very large deposit of sheath saliva. For example, the salivary sheath in Fig. 5a seems to be frozen at the beginning of secreting sheath saliva into a pith cell (Fig. 5a, arrow 3), and the waveform is frozen in the middle of a B2 episode (Fig. 5b).

In fact, a globular sheath saliva deposit somewhere along the length of the sheath was found in 100% of all probes that performed B2 events, not just those terminated during B2. Seventeen of 24 single-branched probes had no B2 (or B2m; see below) event, and the same sheaths also had no bulbous salivary deposit. In contrast, the remaining seven single-branched probes had one or two B2 (or B2m) events each, and all had one or two bulbous deposits, the number of deposits matching the number of events. All 10 multibranched sheaths (six double- and four triple-branched) had at least one B2 (or B2m) event, and all had at least one salivary deposit, usually located at the branch fork(s). The number of salivary deposits was always either the same as, or one less than, the number of B2 (or B2m) events. The number of deposits, or occasionally lumps in a larger deposit, corresponded to the number of B2 events that had been performed (Figure 6c, arrows 3* and 5).

Thus, as with A2 and B1, sheath salivation is associated with B2. This finding is further supported by observations by Joost et al. (2006) who saw copious sheath salivation during B2 in artificial diets (see *Discussion and Conclusions*). This correlation also was pivotal for the interpretation of waveforms discussed in "Case Studies"; see below).

Waveform B2m is correlated with small, bulbous salivary deposits along the length of the salivary sheath, or at the forks of sheath branches. They resemble B2 sheath deposits and are the same size or smaller (Fig. 6a, arrow 2). In fact, the waveform was originally discovered because we observed these very small deposits along the sheath at spatial locations that we hypothesized corresponded temporally with a B2 event but were not marked as such during waveform measurement. When we more closely reexamined the waveform trace, we found the B2m events in every case.

Ingestion Phase: C Waveform. The C waveform family represents continuous ingestion. To determine from which tissues insects were ingesting, and when the insects' stylets first reached xylem, 17 probes were terminated in mid-C and salivary sheaths recovered. Three to four salivary sheaths were recovered from each of the five C event order categories (Table 2). The tips of all 17 sheaths were found to be in empty vascular cells (Fig. 6a, arrow 4). Twelve of the 17

sheath tips (71% overall) were in mature xylem vessel elements.

1stC Waveform Event. Four artificially terminated sheaths were recovered for the first C event, which was performed 29–52 s into the probe (Table 2). The duration of 1stC could be brief ($\approx$10 s) to moderate (80–300 s). In all four cases, the salivary sheaths were single branched and their termini were in vascular tissue (Table 2). Thus, within 1 min of the start of stylet penetration, the vascular tissue was reached for the first time; in 50% of cases, stylets were in a mature xylem vessel element.

2ndC Waveform Event. Three 2ndC events were artificially terminated and salivary sheaths recovered. All sheaths terminated in xylem (unlabeled arrow in protoxylem, Fig. 2c). Probing time to 2ndC was within the first 57–89 s (Table 2). For the first time, we found that one of the three sheaths (5 in Table 2; Fig. 5c) was a multi- (actually double-)branched sheath, whose final branch terminated in a xylem vessel element. This sheath is described at length under "Case Studies." All of the previously mentioned sheaths were single-branched.

3rdC Waveform Event. Three probes were artificially terminated during 3rdC. Two of the three sheaths (i.e., 18, a single-branched sheath and 20, a double-branched sheath) had their final branch tips in xylem vessel elements (Table 2). The first branch of 18 ended in a pith cell, although there is no evidence that ingestion was performed in the first branch. The other single-branched sheath (16) was in "other xylem" (see definition in caption for Fig. 2f). The start of 3rdC occurred more variably late than for 2ndC, from 150 to 272 s into the probe (Table 2). Thus, considering all 1stC to 3rdC events, in six of 10 probes (Table 2), the stylets had reached xylem by 3rdC.

4thC Waveform Event. By 4thC, all four of the artificially terminated, final sheath branch tips were in a mature xylem vessel element (Table 2). Two (8 and 29) left single-branched sheaths; another (13) left a double-branched sheath whose first branch was in phloem; and the fourth (28) left a complex, triple-branched sheath whose first branch tip was in cortical parenchyma and second in a large, saliva-occluded, mature xylem cell. Probing time to this 4thC event was extremely variable, from 136 to 490 s into the probe.

>4thC Waveform Events. Three selections of event orders beyond 4thC were chosen for further correlation via artificial termination (Table 2). Insect 17's probe was terminated during 5thC (not pictured), 26's during 6thC (Fig. 6a), and 10's during 19thC (not pictured). All three of the tips of these insect's final sheath branches were in mature xylem vessel elements when their probes were terminated; two of three (17 and 26) had left three-branched sheaths.

Overall C Event Durations. When all sheath types' C event durations were averaged (Table 3, all sheaths combined), they were found to be longer with increasing order in the probe. However, C event durations also became much more variable (as shown by standard deviations, Table 3) with increased probe duration and event order. Beyond 4thC, variability

was very high; probably due in part to our small sample size. However, variability among average C event durations also was partly explained by the branching pattern of the sheath (Table 3, data for single- versus multibranched sheaths). The trend of increasing event duration was shown strongly for both sheath types for the first two to three C events. Thereafter, single-branched sheaths continued increasing in duration. Multibranched sheaths, however, had their longest mean event duration at 3rdC and thereafter declined steeply to much shorter events after 4thC. This is in strong contrast to single-branched sheaths, which were highly significantly longer ($P < 0.001$) by >4thC (Table 3).

Interruption Phase: N Waveforms. The N waveform family represents diverse behaviors that usually occur deep in vascular tissues or en route from one vascular cell to another. Four probes were artificially terminated during N family waveforms, and all four sheaths were recovered. Two probes were disturbed during nonpathway-like N and two during pathway-like NB1.

Waveform N: Both sheath tips were squarely within mature xylem vessel elements. The 1stN event (Table 2, insect 31) was cleanly terminated. It left a single-branched, hollow sheath with its very thin and fragile branch tip just barely breaking the wall of an empty, mature xylem cell, with no stainable saliva in the cell (not pictured). The 2ndN event (Table 2, insect 15) was very similar, although the sheath branch was thicker; again, no stainable saliva was in the empty cell (not pictured). By definition, a 1stN event had to follow a 1stC event, which usually was very short (Table 3). Therefore, it is likely that both the N and C events occurred in the same xylem cell. This observation, plus the higher electrical conductivity of the N waveform compared with C, suggests that irregular, nonpathway N represents secretion of watery dispersive saliva (which does not stain with conventional histochemicals) into xylem cells.

Waveform NB1: In two pathway-like NB1 events, the stylets were found secreting sheath saliva into mature xylem cells. The cleanly terminated, single-branched, 4thNB1-ending sheath of insect 33 had a solid branch with a hollow tip extending straight into a mature xylem cell (Fig. 2d; Table 2). This final 4thNB1 event was preceded by a short 4thNA2 event within the same interruption phase. In insect 30's sheath (Fig. 6d), the final waveform event was classified as N, i.e., exhibiting no subtype. However, upon closer examination of the waveforms, we found a very short (0.38 s) but unmistakable B1 spikelet burst (three spikes at a repetition rate of 20 Hz.) at the end of 9.0-s long, irregular N event (Fig. 6d, yellow inset box). For statistical summarizing, the event was classified as N, not NB1 (because of our 2.0 s threshold for measurement; see above) (Table 3). Nonetheless, for waveform–sheath correlation purposes, the final disturbed event was clearly B1-like. Therefore, it was listed in Table 2 as 1stN(B1). Interestingly, insect 30's second sheath branch does not terminate in the xylem but in a pith cell (Fig. 6c).

Thus, four cases (of six) have now been identified (i.e., two B1s and two NB1s) where interrupting a B1-like waveform freezes the stylets in the process of secreting sheath saliva. The other two sheaths left evidence of recent copious sheath salivation. This strongly suggests that B1, whether or not it occurred during interruption phase, is correlated with sheath salivation. This supports the conclusion that B1 is performed when the stylets are either moving to a new location in the plant or within the first few seconds after entering a new cell.

Thus, NB1 is similar in appearance and biological meaning to B1. It follows that other interruption waveforms with pathway-like appearances may have biological meanings similar to the original (naming) pathway activities, i.e., that NA1 is probably similar to A1, NA2 to A2, and so on. It is likely, however, that the pathway-like interruption behaviors are performed during formation of second and/or more sheath branches, more deeply in the plant than the original pathway activities that form the trunk and first branch. This hypothesis was tested during the examination of case studies of individual probes, presented below.

Stereotypical Sequences of Multiple Waveform Types and Voltage Levels

Abrupt Voltage Changes. Voltage level (i.e., waveform position) always increased abruptly at the start of a probe and then gradually declined in what seemed to be a logarithmic curve as pathway phase progressed, down to what seemed to be an asymptotic lowest voltage level during ingestion phase. Probes successively terminated at each stage of stylet penetration showed that the deeper the stylets had penetrated (i.e., the longer and deeper the salivary sheath), the lower the voltage level. However, occasionally during this decline, in some probes, either rapid-abrupt or slow-smooth increases in voltage level occurred in mid-probe (Figs. 6b and d, 7d, and 8d). Such probes nearly always left multibranched salivary sheaths in the plant. In such cases, the deeper the sheath branch penetrated beyond a fork in the sheath (especially when those branches were widely separated in the plant tissue), the more abrupt and higher the mid-probe rise in voltage (Figs. 6d, 7d, and 8d). Correlations of stylet activities in artificial diet also showed that stylet depth was inversely proportional to voltage level (Joost et al. 2006). Additionally, Joost et al. (2006) revealed that the stylets often penetrate, retract, and then repenetrate the same branch of the salivary sheath as they move deeper into the substrate. In most cases, each time the stylet is withdrawn, the voltage level increases. This correlation between stylet depth and voltage level holds until the asymptotic lowest voltage level is reached. The closer the voltage level comes to the asymptotic low, the less proportional the correlation with stylet withdrawal, i.e., when the asymptote was reached, the stylet depth could change greatly, but the voltage level changed only a little or not at all (Fig. 8d, insect 32, inset boxes c compared with b).

B2 Episode and Trench. A highly stereotypical combination of waveforms consisted of a short event of B1, followed by a B2 chevron, and then another event of B1. This combination was termed a B2 episode. B2 episodes were sometimes repeated several times in sequence (Fig. 1a, inset). Sometimes, the B2 event was replaced with a B2m event, often (although not always) on a declining voltage level (Fig. 6b); this was termed a B2m episode. Additionally, when the following stereotypical sequence of events occurred, in order, the sequence formed an easily recognizable pattern, termed a B2 (or B2m) trench: 1) mildly declining B1, smoothly transitioning into 2) one to several B2 or B2m episodes, then 3) more steeply declining B1, then 4) a (usually) rapid increase in voltage level, composed of either B1 or A2 (Fig. 6d, arrows 2–4). Sometimes both B2 and B2m occurred close together (Fig. 6d). This sequence was termed a trench because of its appearance when it occurred early in the probe (best illustrated in Fig. 6d, arrows 3–5).

When a B2 (or B2m) trench occurred, it indicated branching of the sheath. All 10 of the multibranched sheaths were produced by probes containing B2 or B2m episodes, all but one of which were in the form of trenches. (The one B2-containing waveform trace that lacked a trench [not shown] was very flat overall, with almost no changes in voltage level. This was probably an artifact of low conductivity because of overly loose wiring.) In contrast, most single-branched sheaths (17 of 24) corresponded to probes that lacked B2 or B2m episodes (Fig. 5b). Not every B2 episode occurred in a B2 trench. Seven of the 24 single-branched sheaths were produced by probes with B2 or B2m, but only one of the seven had a very small B2m trench. Thus, 96% of the time, nontrench B2 or B2m episodes indicated extension of the sheath.

The depth of the decline and rise in voltage level during a B2 trench was usually correlated with greater length and divergence of the sheath branches (Fig. 6c). For example, when the voltage increase occurred early in a probe (Figs. 5d, arrow 2; 6d, arrows 2 and 3), it was either small (correlated with very close branching, Fig. 5c) or more typically very large and abrupt (correlated with divergent branching, Fig. 6c). When a voltage increase occurred later in the probe, it was usually very small (because of the log asymptotic voltage levels described above (Fig. 8d, arrow 7).

Summary of Salivation versus Ingestion. Overall, waveform–salivary sheath correlations strongly suggest that secretion of sheath saliva occurs throughout all pathway phase waveforms as well as during pathway-like waveforms of interruption phase. In contrast, no sheath salivation occurs during ingestion phase. Thus, the analogy of pathway and ingestion with the older AC EPG terms salivation and ingestion, respectively, is confirmed. Nonpathway-like waveforms of interruption phase may or may not represent some sheath salivation. Direct correlation of waveforms with watery salivation was not possible, because watery saliva is unstainable by conventional histological methods.

Case Studies of Individual Probes: Interpreting Their Salivary Sheaths and Waveforms

Sheath Landmarks Correlated with Pathway Waveforms. When individual salivary sheaths were examined side by side with the waveforms that were recorded during their formation, it was clear that every sheath was unique and its matching waveforms reflected this uniqueness. Nonetheless, certain spatial and temporal correlations provided a basis for interpreting the overall pattern of the waveforms, at an unprecedented level of detail. These correlations have been thoroughly described above. However because the following case studies hinge on their evidence, they are summarized together here, in order of importance for interpretation of the case studies.

1. B2 waveform events are correlated with obvious, oval-to-round, sheath saliva deposits. This correlation is supported by four probes artificially terminated during B2, whose sheath tips were in large, similar deposits of sheath saliva. Also, all B2- or long-B2m-containing probes had obvious salivary deposits of the same type, whereas all probes lacking B2 lacked deposits. Finally, Joost et al. (2006) observed secretion of copious sheath saliva during B2 maxillary stylet sawing, forming bulbous deposits at the forks of sheath branches.

2. Voltage rises are correlated with partial stylet withdrawal, and voltage declines with stylet progression (Joost et al. 2006). Also, voltage rises (especially when part of B2 [or B2m] trenches) occur almost exclusively in multibranched probes, representing stylet withdrawal before rebranching. With the exception of the probe of insect 32, described below, the longer or more highly separated the branches, the larger the rises.

3. The stylets can penetrate, withdraw, and repeatedly repenetrate the same sheath branch before settling into a cell for sustained ingestion (Joost et al. 2006).

4. The B1 waveform was performed in almost any tissue along the pathway to and in the xylem.

5. Sheath salivation occurred only during pathway-like waveforms (Joost et al. 2006).

6. No sheath salivation occurred during waveforms C (ingestion) or N (nonpathway-like interruption). All sheath tips of probes terminated during these waveforms were in empty cells.

7. Waveform C (ingestion) was correlated most definitively with sheath tips in vascular cells, deep in plant tissue.

With these correlations in mind, and especially also the structure of the salivary sheath, we closely studied the 34 probes. They revealed that every behavioral event in the progression of stylet penetration to the xylem as well as formation of the sheath could be followed in the pathway waveforms. Evidence for this is presented as a series of seven case studies of representative probes, in Figs. 3–8. The case studies are described in order of increasing complexity.

As a note for Figs. 5–8, all salivary sheaths are portrayed with the exterior of the plant to the left and
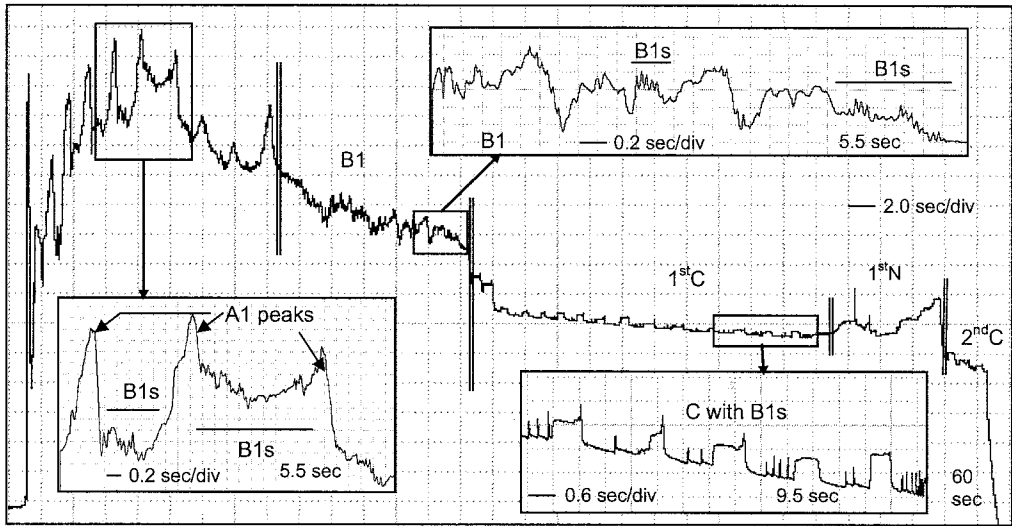
Fig. 3. Waveform trace from insect 7, with inset boxes showing amplified (y-axis) and expanded (x-axis) views of the waveforms to reveal fine-structure detail.

the sheath penetrating inward toward the right. Contiguous sections that contained most parts of each sheath are shown, in order. In like fashion, the corresponding waveforms proceed from left to right. Whenever possible given space available in these figures, waveform traces are labeled with waveform types (double vertical lines) and/or waveform subtypes (thin, single horizontal lines). Branches are labeled with thick horizontal lines. Inset boxes in the waveform traces show amplified (y-axis) and expanded (x-axis) views of the waveforms to reveal fine-structure detail. Landmarks (i.e., corresponding temporal waveform events and spatial sheath structures) are indicated, unless otherwise stated, by corresponding bold numbers in both the waveform and

sheath figures. In all cases except the long probes in Figs. 6b and 7d, the probe ends when the signal abruptly falls to zero. Thus, the entire waveform trace is portrayed for reference. This unfortunately necessitated different degrees of compression for each figure, as indicated by the total duration of each trace (in the right, usually lower corner of each figure).

Single-Branched Sheaths. Fig. 3 shows the waveform trace recorded during formation of the simple, single-branched salivary sheath shown in Fig. 2c of insect 7's probe. The pathway waveforms are short and straightforwardly progress from A1 to B1 to 1stC, interrupted by 1stN, then to 2ndC, during which the probe was cleanly terminated. The voltage level gradually declined to C at about the 50% position, without
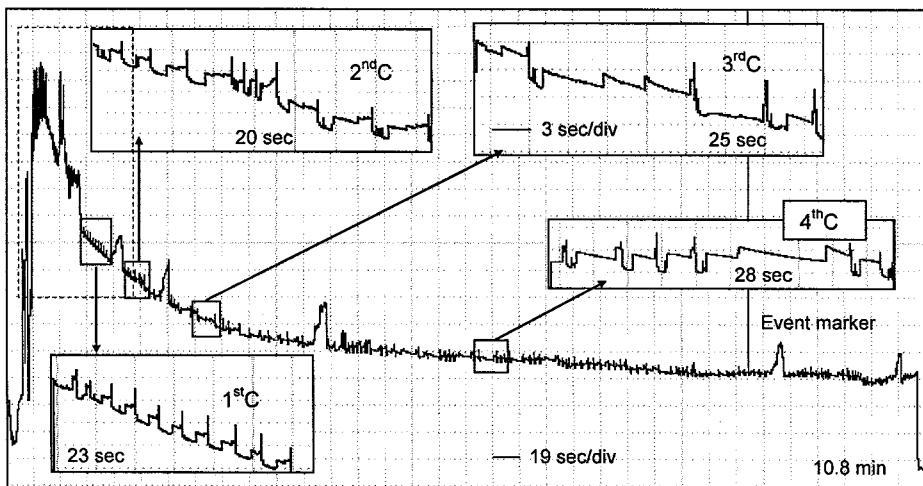
Fig. 4. Complete waveform trace from insect 26, with inset boxes showing amplified (y-axis) and expanded (x-axis) views of the waveforms to reveal fine-structure detail. Expanded view of this probe's pathway and early ingestion phases (dotted box) is seen in Fig. 6b.
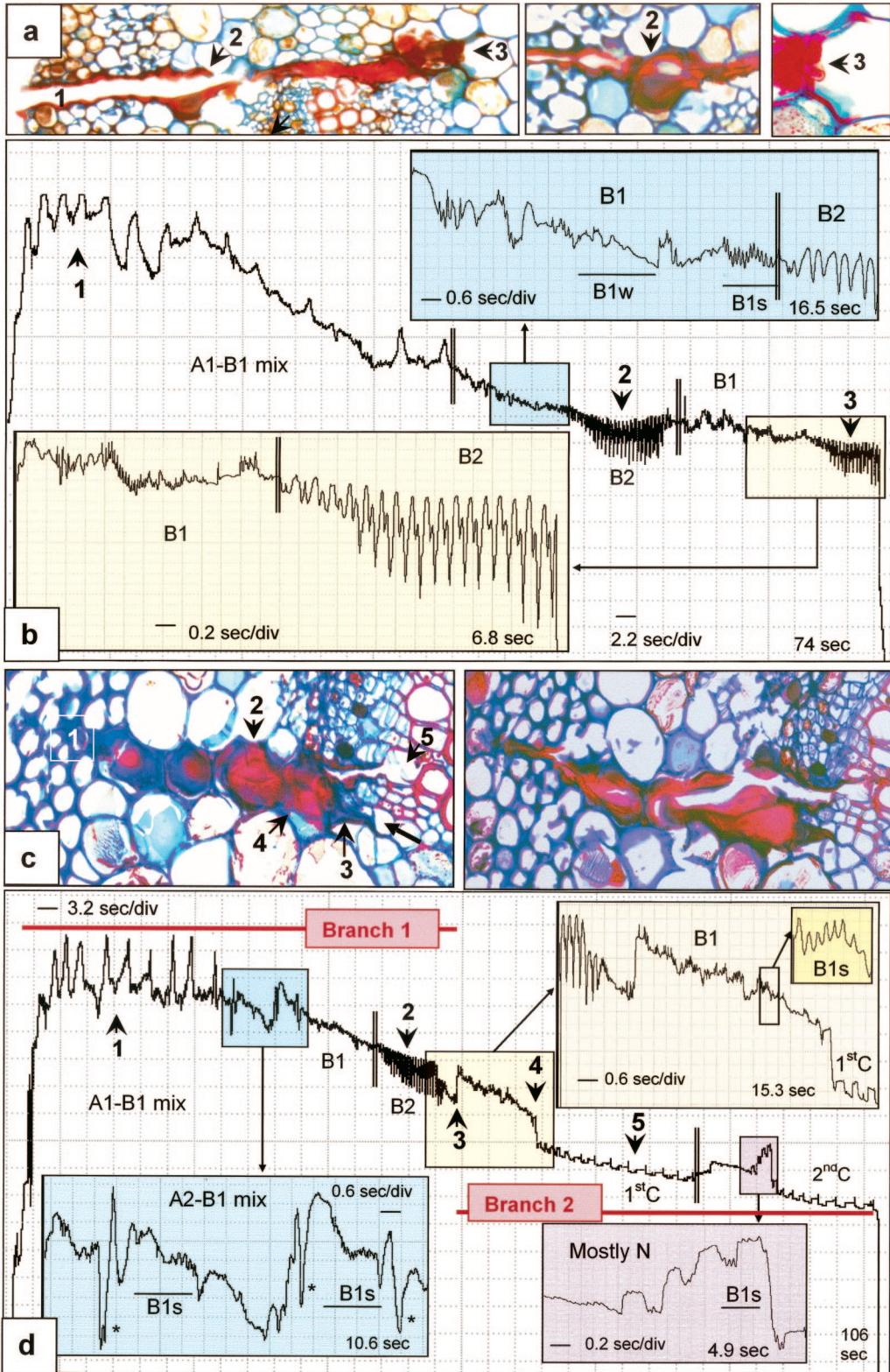
Fig. 5. Case studies of probes by *H. coagulata* 6 and 5, respectively, on susceptible grape petioles. Salivary sheaths images matched with their corresponding waveform traces. (a) Sheath of insect 6. (b) Waveform trace of insect 6. (c) Sheath of insect 5. Un-numbered arrow, cell terminus of first sheath branch. (d) Waveform trace of insect 5. *, rapid voltage decrease.
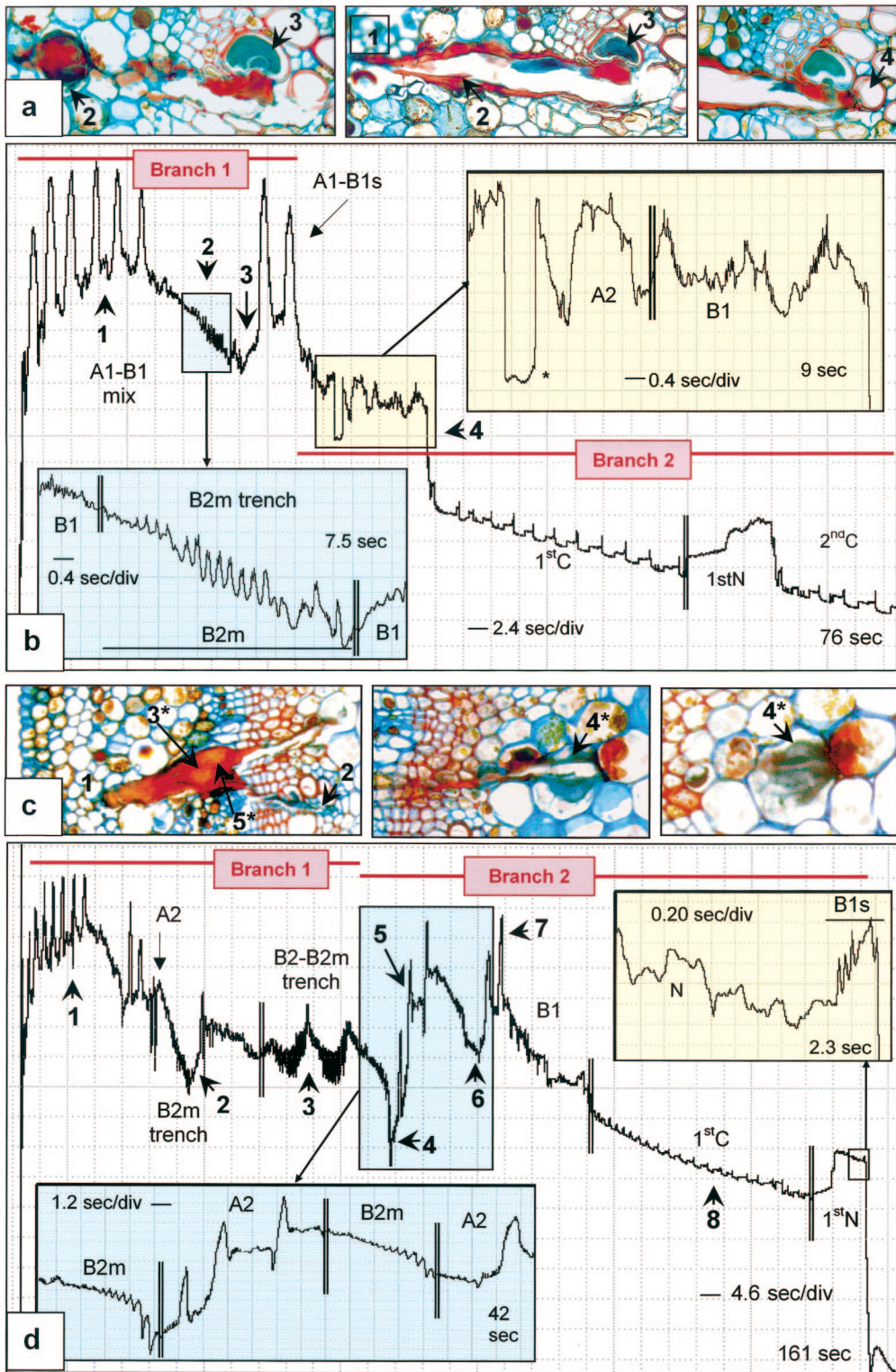
Fig. 6. Case studies of probes by *H. coagulata* 26 and 30, respectively, on susceptible grape petioles. Salivary sheath images matched with their corresponding waveform traces. (a) Sheath of insect 26. (b) Early part of waveform trace of insect 26; the full trace is shown in Fig. 4, in which the portion portrayed in Fig. 6b is boxed with dotted lines. (c) Sheath of insect 30. The second and third images are adjoining sections of the same sheath branch tip. Arrow 4* on the sheath corresponds to arrows 4–8 in the waveform trace, Fig. 6d. d. Waveform trace of insect 30.
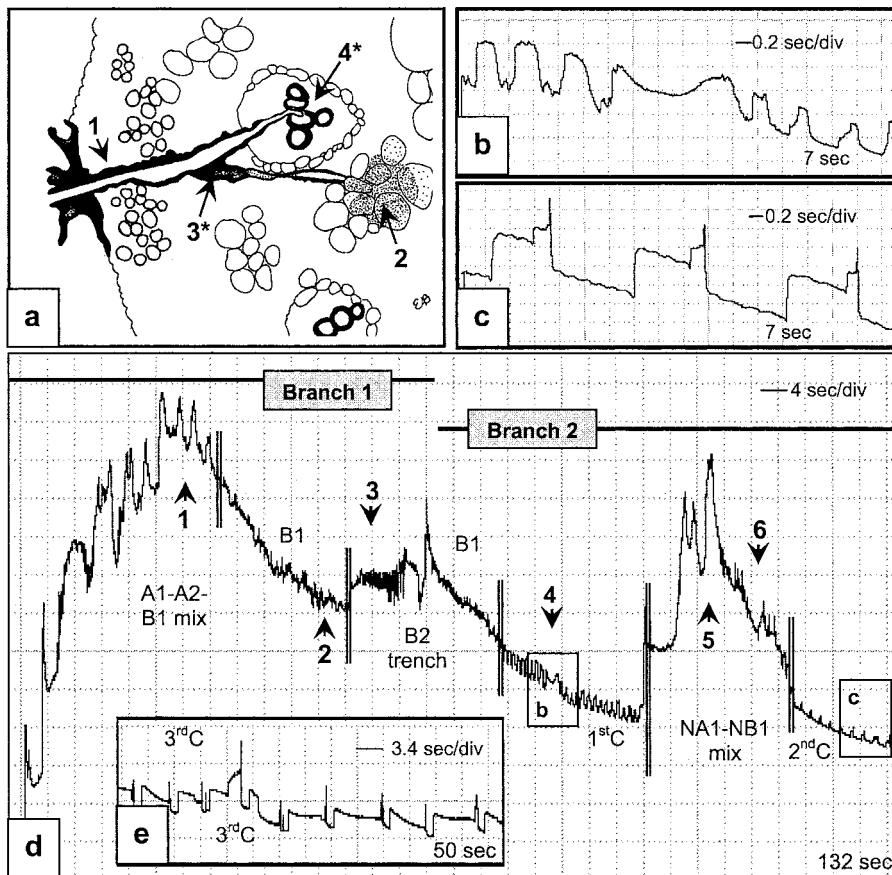
Fig. 7. Case study of probe by *H. coagulata* 20, on susceptible grape petiole. (a) Salivary sheath drawing is an overlay composite of several sections and is matched with its corresponding waveform trace. Arrow 4* on the sheath corresponds to arrows 4–6 in the waveform trace, Fig. 7d. (b) Amplified (y-axis) and expanded (x-axis) view of unusual 1stC, to reveal fine-structure detail. See inset box b in d. (c) Similarly amplified (y-axis) and expanded (x-axis) view of more typical 2ndC. See inset box c in d. (d) Overall waveform trace of insect 20. (e) Appearance of later 3rdC.

abrupt rises. The thin-walled sheath clearly terminated in a hollow protoxylem cell (Fig. 2c, arrow), from which the 2ndC ingestion event occurred. It is not definitively known whether 1stC terminated in the same cell or one preceding that along the pathway. However, the 1stN interruption waveform is simple, irregular and not pathway-like, suggesting that extension of the sheath did not occur during N. Thus, we suspect that both C events occurred in the same protoxylem cell. This probe is an example of a simple, minimal probe straight to the xylem. Minimal pathway activities therefore consist of A1 (sheath trunk formation) and B1 before C (ingestion). Similarly, simple pathway waveforms for probes from two other insects also left simple, single-branched sheaths.

Figure 5a and b (first color plate) depict the waveform trace from insect 6's probe and its corresponding salivary sheath. In this case, the sheath and waveform trace are less simple, although still single-branched. The pathway activities begin with A1 (position [arrow] 1 in the waveform trace, Fig. 5b) and then proceed alternately through B1 and A1 on a gradually declining voltage level, followed by a complete B2 episode (position 2 in the waveform trace, Fig. 5b), continuing into further B1, then begin another B2 episode, which is terminated to end the probe (position 3 in the trace, Fig. 5b). The salivary sheath (Fig. 5a) is more robust and thick walled than the previous sheath from insect 7 and has two large salivary deposits. The evidence supports that the two B2 events correspond to the two large salivary deposits. Therefore, the one in the center of the sheath at the end of the trunk (position 2 in the sheath, Fig. 5a) probably corresponds to the first B2 (position 2 in the trace, Fig. 5b); the one at the tip of the sheath branch (position 3 in the sheath, Fig. 5a) probably corresponds to the second, disturbed B2 (position 3 in the trace, Fig. 5b). The second deposit was interrupted in mid-formation (position 3 in the sheath, Fig. 5a). This is an example of a sheath with a nontrench B2 episode, which represents sheath extension, not branching.

Double-Branched Sheath with Closely Adjoining Branches. Fig. 5c and d (first color plate) shows the sheath of insect 5's probe, with a large salivary deposit
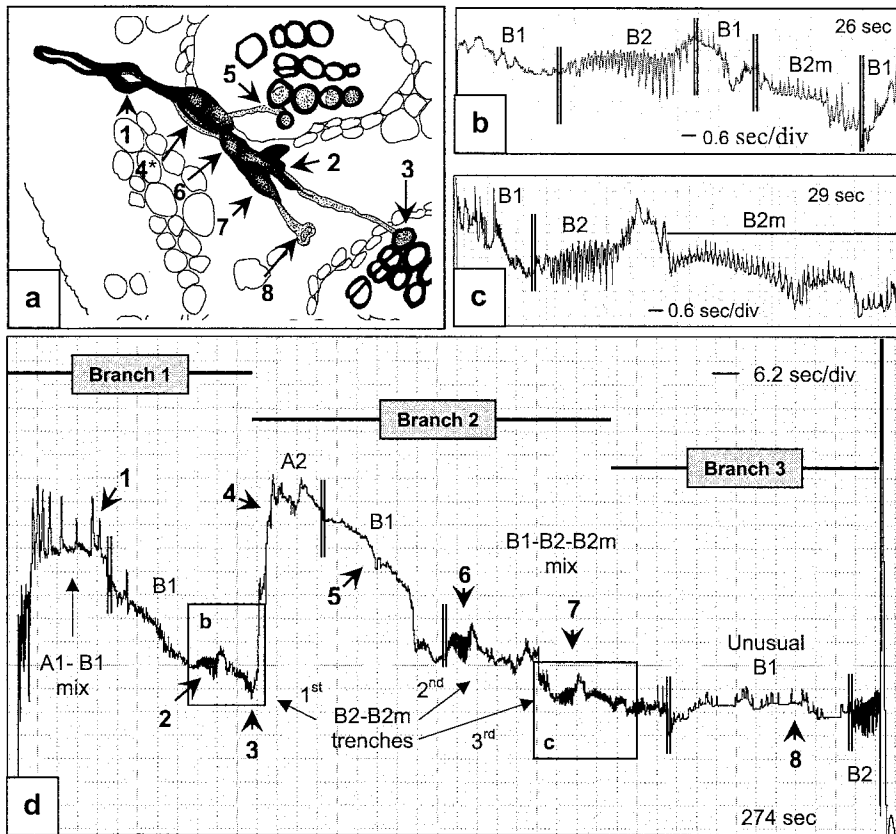
Fig. 8. Case study of probe by *H. coagulata* 30, on susceptible grape petiole. (a) Salivary sheath drawing is an overlay composite of several sections and is matched with its corresponding waveform trace. (b) Amplified (y-axis) and expanded (x-axis) view of B2-B2m trench, to reveal fine-structure detail. See inset box b in d. (c) Similarly amplified (y-axis) and expanded (x-axis) view of flatter B2-B2m trench. (d) Overall waveform trace of insect 30. See inset box c in d.

at the fork of two very short and closely adjoining branches (Fig. 5c). The first branch is filled and terminates in a small interfascicular parenchyma cell just outside a vascular bundle (left sheath image; lower, unnumbered arrow, Fig. 5c). The second branch is clearly hollow, even in part of the large salivary deposit, and perfectly joins a mature xylem vessel element (empty) at its tip (position 5 in the left sheath image, Fig. 5c). The waveform trace (Fig. 5d) begins with A1 (position 1 on the waveform trace, Fig. 5d), then goes on to A2 (expanded in Fig. 5d; blue inset box, including three rapid voltage decreases [*, Fig. 5d, blue inset box] and very short B1 spikelet bursts) before proceeding as usual to declining B1. A somewhat atypical, half-chevron B2 episode occurs next (position 2 in the trace, Fig. 5d), followed by several events (best seen in the yellow inset box, Fig. 5d). The fine structure of the B2 episode in this probe differs from that of the B2 episode in the previous, single-branched probe (position 2 in the trace, Fig. 5b). The B2 of insect number six curves slightly upward, and then proceeds into a flat B1 (Fig. 5b). The half-chevron B2 of insect number five precedes a short B1 spikelet burst and then a small but very abrupt rise in

voltage level (position 3 in the waveform trace, yellow inset box, Fig. 5d), followed by more declining B1. The B2 is in a very shallow B2 trench. An abrupt decrease in voltage level (position 4 in the waveform trace, Fig. 5d) occurs at the start of 1stC (position 5 in the waveform trace, Fig. 5d). 1stC is followed by an irregular, nonpathway N (the end of which is in the pink inset box, Fig. 5d), followed by the 2ndC event that was cleanly disturbed at the end of the probe. The overall voltage level gradually declines to about the 40% position at 1stC. The following interpretation of the salivary sheath best matches, we think, the waveform finding.

The A1–B1 mixture formed the sheath trunk (not shown). As the maxillary stylets exited the trunk and began penetrating deeper (position 1 in the sheath image, Fig. 5c), first the A2–B1 mix, then the B1 were probably performed when the stylets had nearly reached the vascular bundle. The stylets then performed the shallow B2 trench, forming at least part of the salivary deposit (position 2 and neighboring cells in the sheath image, Fig. 5c), out of which they then extended into the parenchyma cell (position 3 in the sheath image, Fig. 5c) during a very brief B1 spikelet

burst (position 3 in the trace, Fig. 5d, yellow inset box, just before the voltage rise). The stylets were then rapidly retracted out of that cell (probably during the abrupt voltage jump, at position 3 on the waveform trace, Fig. 5d), back into the (perhaps) still somewhat liquid salivary deposit (position 4 in the sheath, Fig. 5c), reoriented slightly, and then penetrated a short distance into the xylem vessel element to form the second sheath branch, during the subsequent, downward-sloping B1 event. Within seconds of arriving in the xylem cell, 1stC ensued (Fig. 5c and d, position 5), followed by 1stN and 2ndC. It is definitive that the sheath tip was in the mature xylem cell when 2ndC was interrupted. Because 1stN was nonpathway, we suspect that the stylets merely expelled watery saliva into the cell during N. Therefore, the stylet tips remained at position 5 through 1stC, 1stN, and 2ndC.

Sheath with Double-Branch Tips. Not every double-branched sheath's waveform trace exhibited a clear B2 chevron in its trench. But such an absence always corresponded with an unusual-looking sheath. For example, insect 26's probe (Figs. 4 and 6a, b, second color plate) had a very simple pathway trace (dotted box in Fig. 4, expanded in Fig. 6b). It began with a typical A1 event (with interspersed brief B1 events) that probably formed the sheath trunk (position 1 in the second sheath image, Fig. 6a; actual trunk not shown, because it was in an adjoining section). Then a declining B1 event followed (Fig. 6b), that probably corresponded with the start of the first sheath branch (Fig. 6a). But at the bottom of the B1 decline, instead of an elaborate B2 trench, a short but clear-cut declining B2m event occurred (Fig. 6b, blue inset box). We postulate that, after the declining B1, the stylets sawed through some tough cell walls and/or some hardened sheath saliva on their way inward, during the declining B2m, leaving a small, distinctly round salivary deposit (Fig. 6a and b, position 2), halfway between the sheath trunk and the vascular bundle. At the depth of the B2m trench, they penetrated to the deepest site in the first branch, into a mature xylem vessel element (position 3 in the sheath, Fig. 6a; matching the voltage decline at position 3 in the trace, Fig. 6b). But they did so obliquely, from the side (position 3 in the sheath, Fig. 6a), because the bluish sheath saliva seems to flow into the cell at a right angle to the axis of the sheath. Perhaps this oblique insertion negatively affected the seal of the stylets into the cell, because soon thereafter they apparently retracted back into the first branch, during the abrupt rise in voltage that completed the B2m trench (voltage rise at position 3 on the waveform trace, Fig. 6b). The voltage rise progressed into a second waveform hump, with A1 salivation peaks (Fig. 6b). During this, the stylets were probably retracted partway back into the sheath branch, secreting saliva during A1 both to fill the xylem cell and to thicken/strengthen the walls of the branch.

The second sheath branch began after the second A1 peak on the second hump, as the stylets returned to their inward progression and the voltage level again began to decline (Fig. 6b). For most of its distance, the second branch penetrated the same path as the first, during declining B1 and an elaborate A2 with a rapid voltage decrease (Fig. 6b, *, yellow inset box). Sometime during the following B1 event (also shown in Fig. 6b, yellow inset box), the stylets diverged slightly from the path of the first branch and punctured a second mature xylem vessel element, neighboring the first (position 4 in the sheath, Fig. 6a), probably before the steep voltage decrease preceding 1stC (position 4 in the waveform trace, Fig. 6b). The steep drop may be because of cessation of salivation as cibarial pumping and ingestion ensued. There is no indication from the salivary sheath that the stylets moved any further; they probably remained in that cell through the next five C and four N events (Fig. 4), during which the voltage level continued to decline to the asymptotic low. When the probe was terminated and stylets were pulled out during 6thC (Fig. 4), the same cell was left hollow, not occluded with saliva.

Double-Branched Sheaths with Diverging Branches. *Insect 20's Probe.* The correspondence between the B2/B2m trench and sheath branching is further illustrated with insect 20's probe (Fig. 7, black-and-white figure). The sheath trunk was probably formed during initial A1, B1, and A2 events (Fig. 7a and d, position 1). Then, sometime during the first declining B1 event, the maxillary stylets formed the first sheath branch, penetrating around a vascular bundle and into a group of large pith cells (Fig. 7a and d, position 2). During the B1 event, the insect probably tested the cell and then withdrew its stylets rapidly, causing the voltage level to rise (at the double line after position 2, Fig. 7d). They left behind an unusual, very large, hazy bluish staining saliva deposit, similar in appearance to the deposit in the third sheath image of Fig. 6c (see description below). The saliva filled the terminal pith cell and also permeated into several cells immediately surrounding it. The withdrawn stylets then sawed out of the presumably by-then hardened sheath during the shallow but distinct B2 trench, leaving the narrow, bulbous salivary deposit at the base of the first branch, near the fork of the sheath branches (position 3* in the sheath drawing, Fig. 7a). The stylets then diverged ≈45° and penetrated rapidly and directly into a nearby vascular bundle during the next brief, 4.1 s of (first gradually then abruptly) declining B1. The stylets probably then rapidly withdrew during the abrupt voltage increase (an A2 peak after position 3 in the waveform trace, Fig. 7d). The stylets then repenetrated more slowly into a mature xylem vessel element, during the long, declining B1, and stayed in that cell (position 4* in the sheath drawing, Fig. 7a) as the waveform gradually transitioned into a very oddly shaped (seen in only this probe) 1stC waveform (position 4 in the waveform trace, Fig. 7d, enlarged in b) that lasted for 21.6 s. We hypothesize that the odd shape of this C waveform (Fig. 7b) was related to the position of the stylet tips. The tissue around this site was very mushy (therefore difficult to draw), as though the stylets had repeatedly penetrated there, perhaps during the transitional, declining B1. The drawing in Fig. 7a shows our interpretation that the

stylet tips intersected a xylem vessel element from the side, because the cell wall is sharply broken on that side. Perhaps as a result, the stylet tip seal was not adequate for proper fluid pumping. After the odd 1stC, the abrupt rise in voltage level again signals that the stylets were withdrawn back to the edge of the sheath trunk (position 5 in the waveform trace, Fig. 7d; position 3* in the sheath drawing, Fig. 7a). The waveform immediately progressed into very clear 1stNA1 and 1stNB1, but no 1stNB2. In concert, no salivary deposit rests at the base of the second sheath branch. Therefore, during this time, the stylets probably directly repenetrated back into the second branch (for a third time), into the heart of the vascular bundle, secreting saliva during NA1 to build a thicker wall that resealed the stylets into the side of the xylem cell (position 6 in the waveform trace, Fig. 7d; position 4* in the sheath drawing, Fig. 7a). This probably provided additional sheath saliva to shore up and strengthen the connection to the cell. Finally a more typical-looking 2ndC waveform ensued (Fig. 7d, the first part of which is enlarged in Fig. 7c; the remainder is seen in Fig. 4). When 3rdC was disturbed 1134 s (23.1 min) later, the sheath branch was almost hollow (although not perfectly, so this probe was not included in Table 2).

Insect 30's Probe. As sheath branching became more complex, so too did the waveforms of the corresponding traces. Recurring themes such as B2 trench-branching, seen in simpler traces, became building blocks for interpreting the most complex traces. The next two interpretations of sheaths and waveform traces are not the only ones possible, but we think they are the most logical and parsimonious explanations of events.

Sheath 30 (Fig. 6c and d, second color plate) was a double-branched sheath with a very large, double-humped salivary deposit at the fork of the two long, strongly diverging branches. The probe began as usual with A1 peaks that probably laid down the sheath trunk (not pictured in Fig. 6c; it was in an adjoining section), ending at position 1 (Fig. 6c and d) just above the vascular bundle. Formation of the first sheath branch is probably represented by declining B1, then alternating A1 and A2, followed by more steeply declining B1. The trace then progressed into a short but distinctly chevron-shaped B2m event at the bottom of the first trench (just before the arrow tip at position 2 in the trace, Fig. 6d). The bottom of the trench probably marks the furthest extension of the stylets into the first sheath branch, whose tip is not pictured in Fig. 6c, but was in a pith cell in a damaged adjoining section. (The broken middle of the branch is at position 2 in the sheath, first image, Fig. 6c.) The voltage level then abruptly rises as the stylets are rapidly withdrawn back to the outer edge of the vascular bundle. Then the signal proceeds on a slightly declining to stable level through B1 into two perfect B2 episodes (position 3 in the waveform trace, Fig. 6d). Perhaps these two B2 episodes created the two lumps of the large salivary deposit (position 3 in the sheath image, Fig. 6c). The next B1 declines steeply into the deepest trench (position 4 in the trace,

Fig. 6d, blue inset boxes). Overall, we termed this sequence a B2-B2m trench. During the steeply declining B1 event that completed the trench, the stylets rapidly penetrated to cut the second sheath branch into a second pith cell for the first time (shown in the second and third sheath images [two sections through the same sheath branch], Fig. 6c, at position 4*). Then, the waveform abruptly rises again into several A2 peaks, during which the stylets probably withdraw briefly back into the perhaps still-soft salivary deposit (position 5 in the trace, Fig. 6d, blue inset box; position 5* in the sheath image, Fig. 6c). This is followed by another declining B1, with a short B2m trench (Fig. 6d, blue inset box, position 6 in the waveform trace). The stylets probably sawed out of the salivary deposit and repenetrated the same branch a second time. Then the voltage level rose into distinct A1 peaks (position 7 on the waveform trace, Fig. 6d; position 4* on the sheath images, Fig. 6c). During the subsequent decline into B1, the stylets may have repenetrated a third time down the same branch (see *Discussion* for further evidence of repenetration). Both the second and third times, the stylets probably moved more slowly, laying down more sheath saliva to make a thicker-walled, second sheath branch into the pith cell. The third declining B1 had a long, irregular B1w event at the end that closely resembles irregular N (present just before the double vertical line but not detailed in an inset in Fig. 6d). Finally, the waveform declines into first C (position 8 on the waveform trace, Fig. 6d; position 4* on the sheath images, Fig. 6c) for 40.6 s, before the final event of an irregular 1stN disturbed in the middle of the very brief 1stN(B1) (Fig. 6d, yellow inset box). As already described, the stylets were then pulled out in the act of secreting saliva into the pith cell (position 4* in the sheaths, Fig. 6c).

Triple-Branched Sheath with Highly Divergent Branches. The most complicated waveform trace corresponded with the most complicated, multibranched salivary sheath, from insect 32's probe (Fig. 8a–d). The probe began with a typical signature of alternating A1 and B1 events that formed the sheath trunk (Fig. 8a and d, position 1). A short B2m event (not enlarged in the waveform trace, Fig. 8d), may have formed the first (and smallest) of three salivary deposits (hollow, at the tip of the trunk; position 1 in the sheath drawing, Fig. 8a). The waveform trace proceeded into a long, declining B1 that started the inward penetration of the maxillary stylets. This led next to the first B2/B2m trench (position 2 in the waveform trace, inset b, Fig. 8d, enlarged in b), which we hypothesize corresponded with at least one lump in the third salivary deposit (position 2 in the sheath, Fig. 8a), because that deposit is closest to the longest, probably first, branch. The subsequent, very low-voltage level suggests deep penetration, probably to a mature xylem vessel element in a distant vascular bundle (position 3 in the sheath, Fig. 8a and the trace, Fig. 8d, box b, enlarged in b). The immediately following, very large and abrupt voltage increase (which very unusually represented the 100% position for this probe) (position 4 in the waveform trace, Fig. 8d) suggests that the stylets

were rapidly retracted a long distance (possibly to the second salivary deposit, at position 4* in the sheath drawing, Fig. 8a). As they exited the distant vascular bundle, the stylets secreted bluish-staining saliva that occluded the xylem cell (position 3 in the sheath drawing, Fig. 8a).

The second branch began with a very high-level, stable A2 after the voltage increase. This was followed by a long, steadily declining B1 (position 5 in the waveform trace, Fig. 8d), until an abrupt drop into a B1s event. The salivary sheath suggests that the stylets formed a second branch during the declining B1. But this time, the stylets diverged into a mature xylem vessel element in a nearer vascular bundle (position 5 in the sheath drawing, Fig. 8a), perhaps tapping into it at the instant of the voltage drop. The brief B1s event afterwards thus occurred in the xylem cell. However, once again the stylets remained only fleetingly in that cell. During the later part of the short B1 event (after the drop), the stylets may have then retracted along the branch bore (to position 4* in the sheath drawing, Fig. 8a), although we did not see a rise in signal, as would be expected. In fact, the rest of the pathway is at a very low, stable voltage level. This is the only sheath of the 34 that exhibited this (see further discussion below). Upon retraction, the stylets filled the penetrated xylem cell and adjoining cells with bluish saliva as they exited (position 5 in the sheath, Fig. 8a). The waveform trace then led to the second B2-B2m trench (position 6 in the waveform trace, Fig. 8d) that might correspond with another lump in either the second or third, multilump salivary deposit (position 6 in the sheath, Fig. 8a). The salivary sheath structure suggests that the stylets again returned to the original path and, during the second B2-B2m trench, the stylets sawed through the deposit(s). The waveform trace then proceeded to yet a third B2-B2m trench (position 7 in the waveform trace, Fig. 8c and d, inset c, enlarged in c), at the start of an unusually long series of B2 and B2m episodes. The appearance of the sheath and waveforms suggests multiple sawings and salivary deposit formation as the stylets forced their way through a length of previously solidified sheath saliva, partway along the first branch, and then into a third, new branch. This left a series of several lumpy deposits (positions 4*, 6, and 7 in the sheath drawing, Fig. 8a). The waveforms occurred at such a low voltage level that only a relatively small voltage increase occurred in the trenches, even though the structure of the salivary sheath suggests that this third set of B2-B2m episodes partly corresponds to a long third sheath branch. We hypothesize that the low voltage level could have been because of repenetration into the very thick deposits of sheath saliva that might have insulated the stylets from the applied plant voltage, and/or the log asymptotic voltage level. This third branch points in the direction of the xylem in the distant vascular bundle. Unfortunately, the tip of this third branch was lost, because it was in a damaged, contiguous tissue section. (Position 8 in the sheath drawing, Fig. 8a, marks the cell where the known portion of this branch ends.) Therefore, we cannot

know which type of cell the third branch terminated in, except that a very long (85 s), stable event of a very unusually shaped B1 (or B1-like waveform) (position 8 in the waveform trace, Fig. 8d). The signal then proceeded into yet another B2 event, which was disturbed to terminate the probe.

Clues from Less Definitive Sheath Terminations. Several sheath branches that were naturally terminated before the final, hollow (i.e., artificially terminated) branch were tentatively correlated with pathway waveforms, in the manner described in the case studies above. Although these branches were filled (thus their correlations were not definitive), they nonetheless provide provocative clues about cell types penetrated during certain waveforms. One B2 was terminated in a phloem cell, suggesting that stylet movement (i.e., sheath branching) can occur through nonxylem vascular cells. One 1stC and one 3rdC both were terminated in other xylem, whereas two other 3rdC and 4thC events both were terminated in occluded, mature xylem vessel elements. This supports previous correlations that early C events are often not in a mature vessel, or for some reason, the stylets can abandon a vessel after a brief C event. Most interestingly, two B1 events were terminated in mature xylem vessels, whereas a third was terminated in a pith cell. Although not definitive, this further supports that the xylem probably is penetrated initially during B1, probably for a very brief time before C ingestion ensues.

Waveform Durations and Frequencies for Single-versus Multibranched Sheaths. Most waveform event durations and frequencies were stereotypical and did not differ between probes with single- and multibranched sheaths. However, B1, C (and possibly N) differed between single- and multibranched sheaths. Both the duration (WDE) and frequency (NWEI) of B1 differed. Probes leaving multibranched sheaths had both longer ($P = 0.0416$) and more frequent ($P = 0.0062$) B1 events (Table 4). Also, the mean duration of C (all event orders combined) was significantly much longer ($P = 0.0088$) in probes with single- compared with multibranched sheaths, although the frequency of C events was not different (Table 4). Together, these findings support results from the sheath correlations and case studies, i.e., that B1 is lengthened during sheath branching, whereas less searching (i.e., single-sheath branches) allows longer ingestion (C) durations. In addition, duration of N was numerically shorter ($P = 0.0978$) and frequency of NB1 was numerically less frequent ($P = 0.0926$) for probes leaving single- versus multibranched sheaths. These differences might have become significant with higher sample sizes (TNE). If so, this also describes the greater degree of sheath branching in multibranched sheaths.

Discussion

Waveform Characterization and Correlation

The salivary sheath correlations described herein, as for most EPG correlation studies, were difficult. Although stylet penetration was cleanly terminated in

most cases, it was sometimes not possible to recover the salivary sheath, especially during early pathway waveforms. Therefore, although sample sizes are small, they are quite typical for EPG correlation experiments. Nonetheless, the stereotypical nature of most behaviors represented by the waveforms, combined with confirming data from the case studies, strongly supports our waveform interpretations.

Pathway Phase

Waveform Family A. The early pathway waveforms in this family represent formation of the sheath trunk (A1) and the early formation of the first and sometimes later sheath branches (A2), including penetration through numerous epidermal, cortical parenchyma, and interfascicular and/or pith cells on the way to or past the vascular bundle. Almeida and Backus (2004) first characterized the A family of waveform for sharpshooters in their study of *G. atropunctata.* They designated waveform types A1, A2, and A3. A1 is the same waveform for both *G. atropunctata* and *H. coagulata.* However, the *G. atropunctata* waveforms of A2 and A3 have been recategorized and are now subsumed within just A2, for both sharpshooter species. The two waveform types previously were based on declining versus stable voltage level (Almeida and Backus 2004). However, correlations of sectioned salivary sheaths were not done for Almeida and Backus (2004), and those described herein show that voltage level is explained by stylet depth.

Waveform A1 represents stereotypical stylet activities (Joost et al. 2006) simultaneous with secretion of copious sheath saliva that forms the wide, thick-walled, triangular trunk of the sheath (thus enveloping the entire stylet bundle) and sometimes a thick-walled branch lining later in the probe. Only a small part of the sheath is made in the first one to three peaks of A1, in the first 3 s of a probe. Sheaths were not recovered from six of seven probes that were artificially terminated in early A1, suggesting that all early sheaths are similarly small, incomplete, and not firmly rooted in the plant tissue. The missing sheaths were probably dislodged during the histological preparation process.

The low amplitude of most of waveform A2 suggests that it represents the beginning of slow, delicate penetration of tissues beyond the sheath trunk, perhaps with sheath saliva secreted during the A2 peaks. Very rapid, brief voltage declines during A2 also occur, but their meaning is unknown at this time.

Waveform Family B. These late pathway waveforms represent extension and completion of an existing sheath branch as well as divergence and creation of new sheath branches. The stylets are clearly searching for xylem and the insect is decision-making during this portion of pathway phase.

Waveform B1 can occur in virtually any plant cell. Our study found that one of its subtypes, B1s (spikelet burst), is unique among sharpshooter waveforms in being virtually ubiquitous during stylet penetration, especially during pathway and pathway-like interruption waveforms, but also intermittently at times during ingestion phase. B1 spikelet bursts also were seen in *G. atropunctata* waveforms (Almeida and Backus 2004), but they were not recognized as a separate but ubiquitous waveform type; instead, they were subsumed within all other waveforms, especially A2 and A3 (now redefined more narrowly as the new A2; see above). Although the occurrence of B1s in the valleys between A1 peaks was not observed and discussed in Almeida and Backus (2004), it was accidentally overlooked at the time. Recent reexamination of that previous studies' recordings showed that, indeed, spikelet bursts were intermittently present during *G. atropunctata* A1 (E.A.B., personal observation).

Joost et al.(2006) found that B1s was occasionally (but not consistently) correlated with minute fluttering of the maxillary stylet tips, and slight diminishing of the size of newly secreted globs of still-liquid sheath saliva, possibly because of retraction of saliva into the food canal, or hardening of the saliva. However, each spikelet was not perfectly synchronized with each maxillary flutter. Therefore, some other, physiological process not externally visible probably causes B1s. They suggest that spikelet bursts may represent (at least in part) contractions of the precibarial valve muscle (Backus and McLean 1982, 1983; Backus 1985), either through direct recording of muscle potentials or recording of resulting changes in resistance to applied signal. This hypothesis is being further tested through electromyography and other means. If it proves correct, this would explain why B1s is ubiquitous. The valve is thought to actively function in facilitating fluid uptake into and expulsion from a portion of the precibarium, including tasting of plant cell contents by the precibarial chemosensilla (Backus and McLean 1982). This occurs during a process controlling fluid movement that has been conflictingly termed egestion (Harris 1977, Harris and Harris 2001) or extravasation (McLean and Kinsey 1984). The valve is also thought to passively prevent backflow of fluids into the plant by acting as a pressure-sensitive check valve after contraction of the cibarial dilator muscles that control cibarial pumping and therefore ingestion (Backus and McLean 1982, 1983; Backus 1985). Our findings support that B1s plays a role in decision-making during stylet penetration, because B1s is a part of the B2 or B2m trench (see below), which is correlated with sheath branching and stylet searching. During late-pathway B1 events that occur before ingestion (C) ensues, xylem cells may be approached and penetrated, and their vicinity is tested sensorially.

Waveform B2 represents a highly stereotypical motor program for a previously undocumented leafhopper behavior, "maxillary stylet sawing," accompanied by swirling secretion of sheath saliva (Joost et al. 2006). The artificial diet observations of Joost et al. (2006) showed clearly that a large deposit of sheath saliva was made during B2, as the stylets pivoted and changed direction while salivating. Thus, B2 occurs when the insect is either sawing its way out of its own hardened salivary sheath, or sawing through particularly tough, woody plant tissues. B2 is also performed

by *G. atropunctata* and is designated waveform B in Almeida and Backus (2004). If the meaning of B1 includes precibarial valve movement and sensory testing (see above), then the performance of B1 before and after a B2 event (in a stereotypical waveform sequence we termed a B2 episode) suggests that a highly stereotypical, tasting-sawing-tasting behavior frequently occurs as a course-correcting assessment of sensory stimuli in mid-probe. Such a behavior could be followed by either stylet extension in the same direction or changing stylet direction, causing branching of the salivary sheath.

The fortuitous correlation of B2 events with expanded salivary deposits in the sheath provided a crucial landmark in EPG recording of sharpshooter stylet penetration. In fact, the B2-saliva deposit correlation was so strong that it allowed us to discover the even more frequent (although very short-duration) B2m waveform. Although there was no deliberate disturbance of B2m events for histological correlation, their appearance, position and salivary deposit correlation strongly suggest that they represent a less vigorous form of stylet sawing and sheath salivation. Thus, B2 provided the first step in a logic chain that led to a level of detail in waveform interpretation unprecedented for leafhopper EPG, culminating in the step-by-step descriptions presented in the case studies described above.

Ingestion Phase

Waveform Family C. This waveform family represents ingestion, defined as the uptake of fluid past the true mouth (which in hemipterans is found deep within the head, at the opening of the esophagus after the cibarium), and caused by the rhythmic pumping of the cibarial dilator muscles (Backus and McLean 1983, Backus 1985). During ingestion, large quantities of liquid food are taken up into the precibarium, then cibarium, then "swallowed" into the esophagus and beyond. Although present evidence suggests that some fluid enters the stylet food canal and precibarium during performance of other, preingestive waveforms such as B1s, the quantity of fluid is probably very small and sufficient only for gustatory, not nutritional, purposes. Therefore, only waveform C represents fluid uptake past the true mouth, into the esophagus, midgut, and later reaches of the alimentary canal.

G. atropunctata's waveform family C manifested several small, subtle variations in appearance, leading to designation of two major types (C1 and C2) (Almeida and Backus 2004). However, *H. coagulata* performed many more subtypes of C. Rigorous cataloging of C subfamilies and their correlation with, for example, possible ingestion in different cell types (i.e., phloem versus xylem) or length of time spent ingesting, will require higher sample sizes. Such a study was not in the scope of the present work. Therefore, *H. coagulata* waveform C was not given subfamily (i.e., type) designations at this time.

Crane (1970) and Almeida and Backus (2004) previously correlated the sharpshooter C waveform with ingestion. Both studies described the feeding of the *G. atropunctata*, called *Hordnia circellata* Say in Crane (1970). As summarized in detail in Almeida and Backus (2004), Crane (1970) separated *G. atropunctata* ingestion waveforms into trial ingestion (TI) and sustained ingestion (SI) events, depending upon event duration. TI events usually lasted 20–30 s (always <2 min) and SI events lasted longer. Although the fine structure of *H. coagulata* ingestion waveform C seems slightly different from that of *G. atropunctata*, the findings of Crane (1970) and Almeida and Backus (2004) are remarkably similar to ours. The description of Crane (1970) of TI events corresponds to our early C events, e.g., 1stC, 2ndC, and 3rdC. We do not advocate naming a waveform for a proposed purpose, such as trial versus sustained behavior, hence our more operational, alphabetic waveform names. Nonetheless, it seems that the assessment of Crane (1970) is at least partially correct, i.e., that short-duration ingestion events can be used by the sharpshooter as a means of testing the suitability of the cell, or perhaps the quality of the stylets' attachment to the cell. Our hypothesis of what may occur at this time is discussed under "Summary: Story of a Probe as Represented by EPG Waveforms" (see below).

The combined findings of Crane (1970), Almeida and Backus (2004), and the present work suggest that (at least on susceptible grape) *H. coagulata* ingestion has a very high probability of being from a mature xylem vessel element by the 4thC event (i.e., within the first 3–5 min). If the xylem is successfully reached within the first three C events, the probability is very high that ingestion will continue for a significantly longer duration than if it takes more than three C events to find and accept a xylem cell. If, for some reason, the stylets have less success locating, accepting and ingesting from a mature xylem cell, then more searching for a "proper" xylem cell is occurring. In that case, the overall duration of ingestion is significantly lower during >4thC events.

Future studies may show that ingestion from different tissues can be definitively correlated with different waveform types, subtypes, event order, or durations. If so, then ingestion from xylem versus nonxylem tissues will be identifiable with very high accuracy in real-time, within seconds of its occurrence. Until this possibility is tested, we must continue to use histology (or rate of excretory droplet secretion, which occurs well after onset of ingestion; E.A.B., personal observation) to definitively identify xylem ingestion.

Interruption Phase

Waveforms in this phase interrupt the continuous production of C ingestion waves and therefore occur deep in the plant tissues after the initial sheath trunk and early branch formation. The nonpathway-like waveform (N) probably occurs in the same ingestion cell of the preceding C event, whereas pathway-like

waveforms (NA1, NA2, NB1, NB2, and so on) probably occur after the stylets have exited an ingestion cell and are en route to another.

Waveform N. Three properties of this waveform type suggest that the insect is injecting watery saliva into the cell during this interruption: 1) the usually irregular, wavy appearance of this waveform; 2) its relatively large absolute amplitude (implying electrical conductivity); and most importantly, 3) the empty appearance of correlated cells that are not filled with occluding sheath saliva. We hope to test this hypothesis in future work. If it proves true, perhaps the insect is salivating as a means of combating plant defenses mobilized in the cell in the early stages of penetration, or to dissolve physical blockages of the cell and improve fluid uptake. To date, we have not rigorously categorized and named any waveform types among these irregular events, but it may be possible in the future.

Pathway-Like N Waveforms. Individually, these N waveform types probably represent behaviors very similar to those of their namesake waveforms during pathway phase. Collectively, however, they probably are slightly different in that they represent stylet extension and/or redirection into new tissues deep within the plant and causing branching of the salivary sheath. The insects are probably in search of new ingestion cells, either because they have not yet succeeded in locating a preferred cell or have rejected an unsatisfactory one.

When pathway-like waveforms occurred in BGSS recordings during the interruption phase (although it was not called that at the time), Almeida and Backus (2004) assigned them the standard pathway designations (i.e., A1, A2, B, and so on). However, that work's conditional probabilities could not then distinguish between pathway-like activities at the beginning of a probe versus those during interruption phase. At the time, there were no biological correlations to suggest that there might be differences between these two sets of pathway-like activities. However, results in this paper now confirm that the two types of pathway waveforms show some important differences in meaning, and therefore justify different family and even phase designations. The N-containing designation will allow future tests of conditional probabilities to take those differences into account.

Stereotypical Sequences of Multiple Waveform Types and Voltage Levels

Partial Stylet Withdrawal. The correlation of a change in voltage level with partial stylet withdrawal was first made (and named such) by Walker and Perring (1994) in AC EPG recordings of whitefly feeding (see also comparison with DC EPG recordings in Walker and Janssen (2000)). Interestingly, partial stylet withdrawal in whiteflies is recorded as a decrease in voltage level on the background of gradually increasing voltage level in the probe. This is the opposite of what is seen with AC recordings of sharpshooters and other auchenorrhynchans, in which the

voltage level gradually declines during a probe and partial stylet withdrawal causes a sudden increase in voltage level. The reason for such a difference between sternorrhynchans and auchenorrhynchans is unknown at this time.

Extension of the stylets, withdrawal, and repenetration into the same sheath branch has been seen in artificial diets during A1, A2, and B1 waveforms, and stylet depth during this process is correlated with voltage level (Joost et al. 2006). Thus, stylet depth correlated with voltage level has been seen in both sternorrhynchan and auchenorrhynchan AC waveforms, but not DC (Walker and Janssen 2000) This suggests that waveform position information, i.e., voltage level information about stylet depth in the substrate, has electrical origins in the resistance (R) component (Tjallingii 1978, 2000; Walker and Janssen 2000), which can be emphasized in AC recordings (Backus et al. 2000).

B2 Trench and Leafhopper X Waves. The B2 waveform is unique in appearance compared with all other known leafhopper waveforms. However, in the form of the B2 trench it bears a striking superficial resemblance to X waves produced by some leafhopper species (Wayadande and Nault 1993). X waves are a reliable indication of phloem sieve element penetration and imminent ingestion by deltocephaline leafhopper species. Deltocephalines have been the subject of most EPG studies of leafhoppers (outside of this study, Almeida and Backus 2004 and Crane 1970). Most deltocephaline leafhoppers do not ingest for long durations from xylem on preferred host plants, nor do they probe hard, woody tissues. We would therefore not expect to see a similar stylet sawing behavior in those species. However, the stylet redirection, sheath saliva secretion for branching, sensory discrimination, and decision-making behaviors during a B2 trench, described above, would be expected to occur before location and acceptance of a preferred ingestion cell, regardless of whether in xylem, mesophyll, or phloem tissues. Therefore, it is plausible that at least some B2 trench-like behaviors (including B1 and partial stylet withdrawal, but absent B2 sawing per se) occur during leafhopper X waves. Perhaps future, fine-structure examinations of deltocephaline waveforms will discern spikelet bursts like those in sharpshooter B1s.

Summary: Story of a Probe as Represented by EPG Waveforms

Here, we blend results from the current study to define waveforms on plants with results from the artificial diet study by Joost et al. (2006).

Pathway Phase. The duration of an *H. coagulata* probe is highly variable; it can last from 20 s to 20 h (F.Y., data not shown). Typically, when a sharpshooter settles down on a plant to feed, it first performs a short series of "test probes," each several seconds to minutes long. These are followed by much longer "ingestion probes," lasting one to several hours (Backus 1985, this study). Solidifying sheath saliva is

secreted with every probe, no matter how short. At the beginning of a probe, the stylet-ensheathing labium is pressed to the plant surface and a blob of sheath saliva is secreted to seal the labium to the plant. This forms the salivary flange, on the exterior of the plant. Before the saliva solidifies, the stylets are pushed through and into the plant.

In general, the stylets penetrate intracellularly, i.e., straight through intervening cells and cell walls, by using the maxillaries-ahead approach for stylet penetration (Backus 1988), during which the mandibular stylets penetrate only shallowly and then are braced in the outer plant tissues. This forms the wide sheath trunk, which houses the whole stylet fascicle. The narrower maxillary stylets then penetrate further on their own, moving out from the tip of the mandibulars and forming the narrower and usually thinner walled sheath branches that reach deeply into vascular and other cell types, from which the insect eventually will ingest. All preingestive behaviors comprise the pathway phase of the EPG waveforms, the most intricate. Pathway includes complex sequences of behaviors such as sheath and watery salivation, rapid and intricate stylet movements, and uptake of fluid to various compartments in the alimentary canal.

For more detail, we return to the beginning of the probe. As the stylet fascicle first begins to penetrate the plant, waveform A1 ensues. Copious sheath saliva is secreted in discrete blobs as the entire bundle coordinately extends and retracts, pushing saliva forward, building the sheath that surrounds the stylets as they penetrate. Stylet extension and retraction is perfectly correlated with the rise and fall of large peaks in the first EPG waveform type, A1 (Joost et al. 2006). During A1, the maxillary stylets penetrate two-thirds to three-fourths their full depth, close to the level of the phloem region in a vascular bundle.

The next pathway behavior corresponds to waveform A2, a highly variable waveform that can last a few seconds to 1 to 2 min, or (less commonly) not occur at all. We suspect that lengthening, hardening or polishing of the sheath occurs, along with cell membrane breakage. Together, A1 and A2 represent the formation and completion of the salivary sheath trunk as well as probably significant secretion of watery saliva.

Then, the maxillary stylets, braced by the mandibular stylets and the hardened sheath trunk, begin to penetrate more deeply, still secreting small amounts of sheath saliva. As these narrower, smoother stylets (interior to the mandibular stylets) penetrate further, they secrete a thin-walled sheath branch on the way, and the waveforms progress through A2 and into B1. B1 is an important and ubiquitous waveform that comprises many behaviors, including rapid stylet penetration down to the vicinity of and penetrating into a target ingestion cell. The stylets then often retract, and either the stylets branch in a new direction or the original branch path is repenetrated more slowly to build up the branch walls with further secretion of sheath saliva during waveform subtype B1w. Sometimes, the stylets repenetrate repeatedly down the same branch path.

B1 also represents a major decision-making step in stylet penetration and therefore probably deploys sensory systems such as stylet mechanosensilla (Backus 1985), possible stylet chemosensilla (the papillae on the stylet tips discovered by Leopold et al. 2003) and the precibarial chemosensilla discussed by Backus and McLean (1982, 1983) and Backus (1985). The latter sensilla are probably used during all stages of stylet penetration, but they play an especially important role during B1. Waveform subtype B1s (spikelet bursts) occurs throughout stylet penetration, i.e., during B1, but also interspersed between and among other waveforms. We suspect that spikelet bursts may be involved in tasting by the precibarial chemosensilla, because Joost et al. (2006) showed that although the stylet tips flutter during B1s, the flutter does not always occur, nor is it always perfectly synchronized with B1s spikelet bursts. Therefore, some internal process (perhaps precibarial valve movement) also must occur simultaneously. Early B1 (artificially terminated during our sheath correlation studies) usually occurs in parenchyma, pith, or phloem cells. Whenever B1 is not directly followed by C (ingestion) (see below), we suspect that nonxylem cells are tested and rejected. Later B1 (not artificially terminated during, but inferred from our case studies) often occurs in xylem cells. If a potential ingestion cell is rejected during B1s testing, the insect either withdraws its stylets into the sheath branch, or extends the branch into other cell types.

When the insect withdraws, it often must contend with newly hardened and solidified sheath saliva along the branch. If so, it deploys another B family waveform, B2, which represents maxillary stylet sawing. Highly stereotypical, coordinated extensions and retractions of the maxillary stylets (Joost et al. 2006) saw through the hardened salivary sheath, to make a new branch in a different direction or, sometimes, a forward extension of the sheath. A stereotypical waveform sequence (termed a B2 trench) may be performed, consisting of taste (B1) –saw (B2) –taste (B1) –withdraw stylets (voltage increase during B1 or A2); this marks the formation of a new sheath branch. The stylets then begin a branch in a new direction with either A2 or B1 or both.

Ingestion Phase. Once a potential ingestion cell has been found acceptable, rhythmic pumping of the cibarium ensues, ingestion begins, and the C waveform occurs. Short-duration events of C were almost always in a vascular cell, especially xylem. Of the 14 C events, we disturbed during the first four C events in a probe, only one (a 1stC) was in phloem, the rest (93%) were in some type of xylem (Table 2). Thus, adult *H. coagulata* on susceptible grape ingest almost exclusively from xylem. Yet, it is very possible that this preferred ingestion tissue could change with insect life stage (as suggested by Freeman et al. (2004)) or host plant.

Our research supports the theory of Crane (1970), that early, short-duration C events represent "trial ingestion," and we further hypothesize that the insect is testing the strength of its mechanical seal into the

vascular cell (see further discussion below). The stylets' seal into a xylem cell may be adequate, but the cell can become blocked in some way. Thus, free flow of fluid becomes precluded. The insect then may try to chemically unblock the cell by secreting watery saliva during interruption phase (below). Several iterations of trial ingestion and watery salivation may be necessary to unblock or "prime" the cell. However, if repeated trial ingestion attempts (usually three or four) fail, then the insect will withdraw its stylets, rebranch the sheath, and try to locate a new ingestion cell.

Interruption Phase. Occasionally during ingestion, the C waveform will be interrupted by a highly variable and amorphous group of waveforms, labeled N, interruption. Those portions of nonpathway-like interruption that resemble a variable version of B1w may represent watery salivation into a vascular cell, usually xylem. Pathway-like N represents almost all the same waveforms as described above in pathway phase, and the above-mentioned evidence supports that they have very similar same biological meanings but occur more deeply in the plant. For example, tasting, uptake and expulsion of tiny amounts of fluid into and out of the precibarium (i.e., synonymously, egestion or extravasation) probably occur during NB1; sawing hardened sheath saliva or tough plant tissue occurs during NB2.

When the insect naturally terminates a probe, the maxillaries withdraw to the tip of the mandibulars (the latter still braced in the sheath trunk). In so doing, they secrete sheath saliva (stained blue in our light micrographs) that fills and occludes the terminal plant cell and the sheath branch. The entire stylet fascicle then rapidly is removed without filling, leaving the trunk hollow. This final sheath occlusion can occur during a one- to several-second long event of N; sometimes the event is so rapid and brief that it is termed a pull-out spike. Structure of sheaths left behind in such a manner has been elegantly imaged via light microscopy (Leopold et al. 2003), confocal laser, and transmission electron microscopy (Freeman et al. 2004). The TEM views reveal severe disruption that occurs in xylem cell walls as a result of *H. coagulata* probes as well as the occluding sheath saliva. We agree with the conclusion of Freeman et al. (2004) that blockage to xylem flow and PD-like symptoms could be caused by physical damage and salivary occlusion alone, in *H. coagulata*-probed xylem cells. However, we disagree with those authors' questions regarding the possible function of sheath saliva in sealing stylets into a probed cell and preventing cavitation. Freeman et al. (2004) examined only naturally terminated probes, not artificially terminated probes. Our evidence supports that the stylets do indeed seal themselves into a potential ingestion cell (an idea first expressed by Miles (1968), probably during B1w. Several of our sheath micrographs of artificially terminated probes show saliva just outside of cells as well as closely adhering to the interior of target cells, along the cell wall (Fig. 5a), implying a seal. Also, probes that we succeeded in cleanly disturbing during waveform

C invariably showed no occlusion of xylem cells with sheath saliva (see below), implying free flow of xylem fluid into the stylets. Thus, it seems unlikely to us that cavitation occurs during initial stylet penetration into xylem cells, but perhaps it occurs upon stylet withdrawal out of cells as a result of salivary occlusion.

Implications for Transmission Mechanism of *X. fastidiosa*

Due primarily to the pioneering efforts of A. H. Purcell (one of the honorees of this *Annals of the Entomological Society of America* volume), it has been known for many years that shag carpet-like colonies of *X. fastidiosa* line the precibarium and cibarium of its sharpshooter vectors (Purcell et al. 1979, Brlansky et al. 1983). It has been presumed that the bacteria are somehow expelled into the xylem from this anterior-most area of the foregut (Purcell 1990). Evidence suggests that expulsion of as few as 100 bacterial cells can establish a successful infection in susceptible grape (Hill and Purcell 1995). Yet, no firm evidence exists of exactly how the bacteria are expelled, and at what stages in stylet penetration.

Hypotheses regarding transmission (especially inoculation) mechanisms have centered around the precibarium (Purcell and Hopkins 1996). Backus and McLean (1982, 1983) discovered the precibarial valve in sharpshooters and other leafhoppers. Based on the valve's functional anatomy, they postulated that it acts both to actively compartmentalize two sets of chemosensilla, and as a passive, pressure-sensitive check valve during cibarial pumping/ingestion. Backus and McLean (1983) also broadly suggested that understanding the function of the valve could be important in explaining pathogen transmission mechanisms by vectors. Based on that work, Brlansky et al. (1983) and later Purcell (1990) postulated that valve malfunction because of bacterial clogging (Brlansky et al. 1983) or miscoordination of the valve and the cibarial retractor/dilator muscles (Purcell 1990) during tasting or ingestion could cause bacteria to be expelled from the precibarium. Fereres and Collar (2001) also support such an ingestion–egestion/extravasation mechanism of *X. fastidiosa* transmission, reminding us that sharpshooter food and salivary canals are not fused at the tip of the stylets (also shown by Leopold et al. 2003), as are aphid canals. Thus, the ingestion–salivation hypothesis, considered strongly possible for aphid transmission of noncirculative viruses, is not likely to operate (or at least, not exclusively) in sharpshooter vectors.

Our work may support the role of the precibarial valve in the inoculation mechanism and begins to suggest when during the process of stylet penetration the bacteria are expelled. We have shown that the only EPG waveforms that occur in the xylem are B1, C, and nonpathway N. B1s might represent in part precibarial valve activity and thus be related to *X. fastidiosa* inoculation. However, stronger evidence is certainly needed before we can state that definitively. Ingestion (C) represents the major behavior occurring in

the xylem. Its duration could conceivably be related to *X. fastidiosa* inoculation if every pump of the cibarium requires the pressure-sensitive check valve to function, as suggested by Backus and McLean (1983) and Purcell (1990). Also, B1s occasionally occurs interspersed with C plateaus during C. However, if nonpathway N represents, as we suspect, watery salivation into ingestion cells, then it may not play a role in inoculation if the ingestion–salivation hypothesis proves wrong. Future work will identify more precisely the EPG waveforms representing precibarial valve activity and expulsion of *X. fastidiosa.*

References Cited

Almeida, R., and E. A. Backus. 2004. Stylet penetration behaviors of *Graphocephala atropunctata* (Say): EPG waveform characterization and quantification. Ann. Entomol. Soc. Am. 97: 838–851.

Backus, E. A. 1985. Anatomical and sensory mechanisms of leafhopper and planthopper feeding behavior, pp. 163–194. *In* L. R. Nault and J. G. Rodriguez [eds.], The leafhoppers and planthoppers. Wiley, New York.

Backus, E. A. 1988. Sensory systems and behaviours which mediate hemipteran plant-feeding: a taxonomic overview. J. Insect Physiol. 34: 151–165.

Backus, E. A. 1994. History, development, and applications of the AC electronic monitoring system for insect feeding, pp. 1–51. *In* M. M. Ellsbury, E. A. Backus, and D. L. Ullman [eds.], History, development, and application of AC electronic insect feeding monitors. Entomological Society of America, Lanham, MD.

Backus, E. A. 2000. Our own jabberwocky: clarifying the terminology of certain piercing-sucking behaviors of homopterans, pp. 1–13. *In* G. P. Walker and E. A. Backus [eds.], Principles and applications of electronic monitoring and other techniques in the study of homopteran feeding behavior. Entomological Society of America, Lanham, MD.

Backus, E. A., and D. L. McLean. 1982. The sensory systems and feeding behavior of leafhoppers. I. The aster leafhopper, *Macrosteles fascifrons* Stål (Homoptera: Cicadellidae). J. Morphol. 172: 361–379.

Backus, E. A., and D. L. McLean. 1983. The sensory systems and feeding behavior of leafhoppers. II. A comparison of the sensillar morphologies of several species (Homoptera: Cicadellidae). J. Morphol. 176: 3–14.

Backus, E. A., and W. H. Bennett. 1992. New AC electronic insect feeding monitor for fine-structure analysis of waveforms. Ann. Entomol. Soc. Am. 85: 437–444.

Backus, E. A., M. J. Devaney, and W. H. Bennett. 2000. Comparison of signal processing circuits among seven AC electronic monitoring systems for their effects on the EMF and R components of aphid (Homoptera: Aphididae) waveforms, pp. 102–143. *In* G. P. Walker and E. A. Backus [eds.], Principles and applications of electronic monitoring and other techniques in the study of homopteran feeding behavior. Entomological Society of America, Lanham, MD.

Brlansky, R. H., L. W. Timmer, W. J. French, and R. E. McCoy. 1983. Colonization of the sharpshooter vectors, *Oncometopia nigricans* and *Homalodisca coagulata*, by xylem-limited bacteria. Phytopathology 73: 530–535.

Crane, P. S. 1970. The feeding of the blue-green sharpshooter *Hordnia circellata* (Baker) (Homoptera: Cicadellidae), Entomology. University of California-Davis, Davis, CA.

Ellsbury, M. M., E. A. Backus, and D. E. Ullman. 1994. The history, development and application of AC electronic insect feeding monitors. *In* M. M. Ellsbury, E. A. Backus, and D. L. Ullman [ed.], Thomas Say Publications in Entomology: Proceedings. Entomological Society of America, San Antonio, TX.

Fereres, A., and J. L. Collar. 2001. Analysis of noncirculative transmission by electrical penetration graphs, pp. 87–110. *In* K. F. Harris [ed.], Virus–insect–plant interactions. Academic, San Diego, CA.

Freeman, T. P., R. A. Leopold, and T. J. Henneberry. 2004. Ultrastructural contributions to the study of the glassy-winged sharpshooter and Pierce's Disease, pp. 100–101. *In* 2004 Pierce's Disease Research Symposium. California Department of Food and Agriculture, Coronado Island.

Harris, K. F. 1977. An ingestion-egestion hypothesis of noncirculative virus transmission, pp. 165–220. *In* K. F. Harris and K. Maramorosch [eds.], Aphids as virus vectors. Academic, New York.

Harris, K. F., and L. J. Harris. 2001. Ingestion-egestion theory of cuticula-borne virus transmission, pp. 111–132. *In* K. F. Harris [ed.], Virus–insect–plant interactions. Academic, San Diego, CA.

Hill, B. L., and A. H. Purcell. 1995. Acquisition and retention of *Xylella fastidiosa* by an efficient vector, *Graphocephala atropunctata.* Phytopathology 85: 209–212.

Joost, P. H., E. A. Backus, and F. Yan. 2006. Correlation of stylet activities by the glassy-winged sharpshooter, *Homalodisca coagulata* (Say), with electrical penetration graph (EPG) waveforms. J. Insect Physiol. (in press).

Leopold, R. A., T. P. Freeman, J. S. Buckner, and D. R. Nelson. 2003. Mouthpart morphology and stylet penetration of host plants by the glassy-winged sharpshooter, *Homalodisca coagulata* (Homoptera: Cicadellidae). Arthropod Struct. Funct. 32: 189–199.

McLean, D. L., and M. G. Kinsey. 1964. A technique for electronically recording aphid feeding and salivation. Nature (Lond.) 202: 1358–1359.

McLean, D. L., and M. G. Kinsey. 1967. Probing behavior of the pea aphid, *Acyrthosiphon pisum.* I. Definitive correlation of electronically recorded waveforms with aphid probing activities. Ann. Entomol. Soc. Am. 60: 400–405.

McLean, D. L., and M. G. Kinsey. 1984. The precibarial valve and its role in the feeding behavior of the pea aphid (*Acyrthosiphon pisum*). Bull. Entomol. Soc. Am. 30: 26–31.

Miles, P. W. 1968. Insect secretions in plants. Annu. Rev. Phytopathol. 6: 137–164.

[NRC] National Research Council. 2004. California agricultural research priorities: Pierce's disease. National Academic Press, Washington, DC.

Purcell, A. H. 1990. Homopteran transmission of xylem-inhabiting bacteria, pp. 243–266. *In* K. F. Harris [ed.], Advances in disease vector research, vol. 6. Springer, New York.

Purcell, A. H., and D. L. Hopkins. 1996. Fastidious xylem-limited bacterial plant pathogens. Annu. Rev. Phytopathol. 34: 131–151.

Purcell, A. H., A. H. Finlay, and D. L. McLean. 1979. Pierce's disease bacterium: mechanism of transmission by leafhopper vectors. Science (Wash. DC) 206: 839–841.

Reese, J. C., W. F. Tjallingii, M. van Helden, and E. Prado. 2000. Waveform comparisons among AC and DC electronic monitoring systems for aphid (Homoptera: Aphididae) feeding behavior, pp. 70–101. *In* E. A. Backus [ed.], Principles and applications of electronic monitoring and other techniques in the study of homopteran feeding behavior. Entomological Society of America, Lanham, MD.

Ruzin, S. E. 1999. Plant microtechnique and microscopy. Oxford University Press, Oxford, England.

SAS Institute. 1998. The SAS user's guide. SAS Institute, Cary, NC.

Serrano, M. S. 1997. Probing behavior of the leafhopper *Empoasca kraemeri* (Ross & Moore) on susceptible and resistant cultivars of the common bean *Phaseolus vulgaris* L. University of Missouri, Columbia, MO.

Serrano, M. S., and E. Backus. 1998. Differences in cellular abnormalities induced by the probing behaviors of *Empoasca kraemeri* (Homoptera: Cicadellidae) on tolerant and susceptible common beans. J. Econ. Entomol. 91: 1481–1491.

Serrano, M. S., and Backus, E. A., and Cardona, C. 2000. Comparison of AC electronic monitoring and field data for estimating tolerance to *Empoasca kraemeri* (Homoptera: Cicadellidae) in common bean genotypes. J. Econ. Entomol. 93: 1796–1809.

Sorensen, J. T., R. J. Gill. 1996. A range extension of *Homalodisca coagulata* (Say) (Hemiptera: Clypeorrhyncha: Cicadellidae) to southern California. Pan-Pacific Entomol. 72: 160–161.

Tjallingii, W. F. 1978. Electronic recording of penetration behaviour by aphids. Entomol. Exp. Appl. 24: 721–730.

Tjallingii, W. F. 2000. Comparison of AC and DC systems for electronic monitoring of stylet penetration activities by homopterans, pp. 41–69. *In* G. P. Walker and E. A. Backus [eds.], Principles and applications of electronic monitoring and other techniques in the study of homopteran feeding behavior. Entomological Society of America, Lanham, MD.

van Helden, M., and W. F. Tjallingii. 2000. Experimental design and analysis in EPG experiments with emphasis on plant resistance research, pp. 144–171. *In* G. P. Walker and E. A. Backus [eds.], Principles and applications of electronic monitoring and other techniques in the study of homopteran feeding behavior. Entomological Society of America, Lanham, MD.

Walker, G. P. 2000. A beginner's guide to electronic monitoring of homopteran probing behavior, pp. 14–40. *In* G. P. Walker and E. A. Backus [eds.], Principles and applications of electronic monitoring and other techniques in the study of homopteran feeding behavior. Entomological Society of America, Lanham, MD.

Walker, G. P., and T. M. Perring. 1994. Feeding and oviposition behavior of whiteflies (Homoptera: Aleyrodidae) interpreted from AC electronic feeding monitor waveforms. Ann. Entomol. Soc. Am. 87: 363–374.

Walker, G. P., and E. A. Backus. 2000. Principles and applications of electronic monitoring and other techniques in the study of homopteran feeding behavior. Entomological Society of America, Lanham, MD.

Walker, G. P., and J.A.M. Janssen. 2000. Electronic recording of whitefly (Homoptera: Aleyrodidae) feeding and oviposition behavior, pp. 172–200. *In* G. P. Walker and E. A. Backus [eds.], Principles and applications of electronic monitoring and other techniques in the study of homopteran feeding behavior. Entomological Society of America, Lanham, MD.

Wayadande, A. C., and L. R. Nault. 1993. Leafhopper probing behavior associated with maize chlorotic dwarf virus transmission to maize. Phytopathology 83: 522–526.

Wells, J. M., B. C. Raju, H. Y. Hung, W. G. Weisburn, L. Mandelco-Paul, and D. J. Brenner. 1987. *Xylella fastidiosa* gen. nov., sp. nov: gram-negative, xylem-limited, fastidious plant bacteria related to *Xanthomonas* spp. Int. J. Syst. Bacteriol. 37: 136–143.